
# Technische Universität Berlin

Fakultät I, Fachgebiet Neuronale Informationsverarbeitung


# Comparison of Rate and Phase-of-Firing Code in a Simple Model of the Thalamocortical Feedback Loop

Bachelor Thesis

May 23, 2011


**eingereicht von:** Maximilian Thess 232941 max.thess@gmail.com

**eingereicht am:** 2. Dezember 2010

**Betreuer:** Dr. Malte Rasch, ION Shanghai

Prof. Klaus Obermayer, TU Berlin

# Contents

# List of Figures



# List of Tables

# Acknowledgements

I would like to thank my advisor in Shanghai, Dr. Malte Rasch for the support and guidance he has given me. I also would like to thank Dr. WU Si and his team at the lab of Computational Neuroscience, ION Shanghai for the friendly, welcoming atmosphere and opportunity of broadening my knowledge of computational neuroscience as well as of the Chinese language.

**Abstract**

*Recent findings suggest a special structure of the feedback connections between LGN and V1. Motivated by the fact, that feedback connections can cause neural systems to oscillate and that these oscillations can be used as a reference signal for a phase of firing code, in this thesis a two cell model of the thalamocortical feedback loop is checked for its ability to employ such a code. A simplified rate model is first analyzed to understand the source of oscillations, subsequently a spiking model of integrate and fire neurons is set up and used for transmission of information about the strength of stimuli between one cell lying in LGN and another representing a cell in V1. Factors that influence the ability of the system to transmit information are identified and the performance of the system using a rate and a phase of firing code is compared using measures defined for that purpose. Different configurations of the model that are motivated biologically are tested and mechanisms that can explain their behavior are suggested. It is found that the phase of firing code does not have an advantage over the rate code if perfect discernability of stimuli is necessary, but can reduce uncertainty for stimuli that lie so close together that they are not always perfectly discriminable due to the noisy neural transmission. Besides the strength of the feedback and the amount of noise it is found that the choice of a reference signal and the properties of the decoding window affect the performance considerably. The possible application of a phase code in a more realistic model of the visual system is discussed briefly.*

# Note Added in Proof

Equation 27 on page 37 does not model an I&F neuron with a *standard* self-excitatory synapse. The term $-(g_{\mathrm{fb}}w_{\mathrm{fb}} - g_{\mathrm{ee}}w_{\mathrm{fb}})(U - E_{S_U})$ with $E_{S_U}$ = -80 mV lumps together the effects of the negative feedback from the V-neuron and the self-excitation of the U-neuron, but leads to a non-standard behaviour of the self-excitatory synapse: A standard excitatory synapse would be modelled using a term $-g_{\mathrm{e}}w_{\mathrm{ee}}(U - E_{S_{\mathrm{exc}}})$ where $E_{S_{\mathrm{exc}}}$ is chosen around 0 mV. The self-excitatory effect will in this case *decrease* as the membrane potential $U$ approaches the firing threshold $U_{\mathrm{Th}}$ = -54 mV. For $U = -70mV$ the input current to the neuron is $g_{\mathrm{e}}w_{\mathrm{ee}} \cdot 70mV$, at the threshold it is $g_{\mathrm{e}}w_{\mathrm{ee}} \cdot 54mV$. However, as written in equation 27 and implemented in the numerical simulations the self-excitatory effect of the synapse *increases* as U approaches the threshold. For $U = -70mV$ the input current is $g_{\mathrm{e}}w_{\mathrm{ee}} \cdot 10mV$ at the threshold it is $g_{\mathrm{e}}w_{\mathrm{ee}} \cdot 26mV$.
This may have an influence on the firing patterns of the neurons and therefore the mutual information calculations.

# 1 Introduction

> "But an effect can become a cause, reinforcing the original cause and producing the same effect in an intensified form, and so on indefinitely. A man may take to drink because he feels himself to be a failure, and then fail all the more completely because he drinks."
>
> — George Orwell describes feedback loops in the absence of inhibition.[1]

What role does feedback play in the information-processing in the brain? It is known, that the introduction of feedback in a system of coupled neurons will easily lead to oscillations. Those oscillations are ubiquitous phenomena in the human brain. One hypothesis for neural information coding - the phase of firing code - suggests, that the information carried by spike-trains can be increased considerably if not only their rate, but also their timing relative to the phase of an oscillating reference signal is considered. This reference signal could be created by feedback-induced oscillations. Recent findings suggest, that the feedback between V1 and LGN, two areas in the brain that are involved in vision, has a certain structure, connecting neurons in LGN and V1 that have the same receptive field. Therefore those neurons will oscillate, if they are stimulated accordingly. This thesis will try to show that:

> *A phase of firing code can perform better than a rate code if it takes advantage of the network oscillations that arise in a feedback loop. Structured feedback can therefore have useful applications in the LGN-V1 feedback loop.*

In order to do that, the notion of performance will be clarified using concepts from information theory. The first chapter will give a short introduction to the concepts of (computational) neuroscience, neuronal codes, dynamic systems theory and information theory that are used in this thesis. In the second chapter a simple model of two coupled neurons that represents one neuron in LGN and one in V1 will be analyzed analytically and numerically and its ability to employ a rate of firing and phase code will be looked at. Since it turns out that the vague definitions of rate and phase of firing code allow for many different configurations of the neural system and the decoding method, a number of different possibilities will be tried out. Those possibilities will be motivated mostly by the biological structure the model represents. Relevant properties that are found will tentaively be explained by some mechanisms. The third chapter explores possible applications of the findings for the two-cell-model in a larger network that has more similarities with the real brain.
The topic of this thesis falls into the line of research that investigates the nerual code. Why would one study neural codes at all? The main reason is of course curiousity, the driving force behind research in the natural sciences. Besides quenching the everlasting thirst of researchers, knowing what codes are used by the brain has practical applications, too. Today's artificial limbs and other neuroprosthetics need to communicate with the brain. How does an artificial arm know, that its owner wants to grasp an object? How does a camera, that restores lost eyesight send its images to the brain? Certainly not in the MPEG-format! This can only be done if these artificial devices "understand" (in

[1] See [15].

the case of an artificial arm) or even "speak" (in the case of an artificial eye) the language of the brain. This language is the neural code. Understanding how information is represented and transmitted in the brain is therefore not only an important step towards understanding the brain as a whole but will also help to develop better devices interacting with the human brain.

# 2 Basic Concepts

In this chapter the basic building-blocks of simulations of the brain – neurons and synapses – will be introduced. Mathematical terminology that is used to describe the behavior of dynamical systems will be given. After that, the visual system and a classical model of this system, the Hubel-Wiesel model, will be explained briefly, adding some recent experimental findings regarding the structure of feedback. Two simple models that represent a pair of neurons in LGN and V1 are introduced, a spiking model of I&F neurons is used to analyze them numerically. Before that a rate model is derived from the spiking model that allows analytical treatment and gives hints to a proper setup of the spiking model. Finally the two different types of neural codes that will be compared in this thesis – the rate code and the phase of firing code – will be presented and a measure for evaluating the ability of noisy communication channels, the mutual information, will be given.

## 2.1 Neurons

Different parts of the body are made of different cells, that are specialized for their tasks. While muscle-cells can contract or relax in order to facilitate movement and blood cells bind and transport oxygen, nerve cells relay electrical signals that are widely accepted to be a manifestation of cognitive activity. This part gives a short overview of the basic properties of nerve-cells and simplified mathematical descriptions that are used to model their behavior.

### 2.1.1 Real Neurons

There are about 100 billion neurons in the human brain. Those neurons are made up of three parts, the dendrite, the cell body (also called the soma) and the axon. Their rich behavior emerges from connections to other neurons through synapses. Due to different concentrations of ions (mostly $Na^+, Ca^{2+}, Cl^-$) inside and outside of the neuron a potenial difference (called the membrane potential) exists. Neurons propagate electric signals, called action potentials or spikes. These are sharp increases in the membrane potential. Spikes run through the axon of a neuron that can be connected to a large number of other neurons until they arrive at synapses where they trigger the release of neurotransmitters. These transmitters cross the synaptic cleft (the space between two neurons), arrive at the postsynaptic dendrite and alter the conductivity of its membrane. Depending on the effect synapses have on the postsynaptic neuron ("target") they are called excitatory if they increase the membrane potential of its target (depolarization) or inhibitory if they decrease (hyperpolarization) the membrane potential.[2] The membrane potential typically lies around -60 mV. While dendrites can only passively relay electrical signals, axons are able to amplify voltage changes and are therefore able to transmit them over longer distances without attenuation. Sub-threshold increases in the membrane potential decrease fast in time and space.
Neurons receive input from a large number (up to 100.000) of other neurons that all connect to its dendrite; incoming spikes increase or decrease their membrane potential. Each neuron has a certain threshold, that is determined by the type of the cell as well as its history. If the combined influence of the incoming spikes crosses that threshold, the

[2] A detailed description of synaptic processes can be found in [18].

neuron fires a spike. Shortly after a spike has been fired, no second spike can be fired, this period is called refractory period.

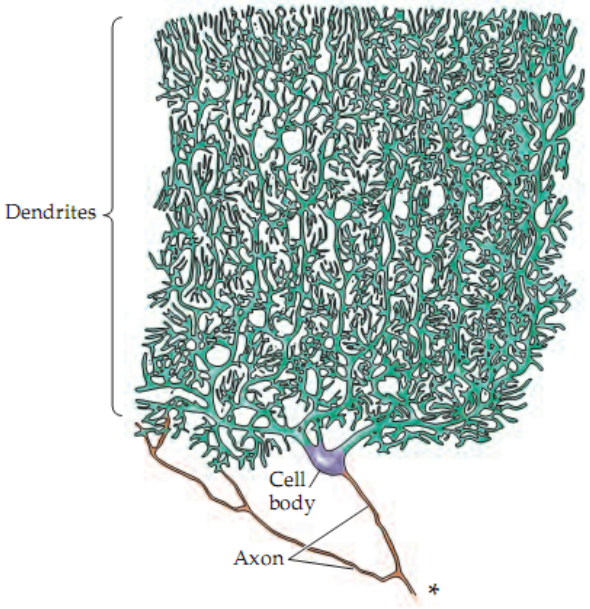


Figure 1: Schematic representation of a cerebellar purkinje cell, from [18]. The cell body of a neuron is about 10-50 $\mu m$ in diameter.

The quick changes in the membrane potential are made possible by small channels in the membrane of the cell, that control the influx or outflux of ions. The creation of spikes is determined by the way in which ions flow in and out of the cell. These mechanisms have been studied in detail by Hodgkin and Huxley[3], who developed a simplified mathematical model of the dynamics of the ion channels that could reproduce the creation and shape of action potentials to an astonishingly accurate degree.

### 2.1.2 Model Neurons

In the Hodgkin-Huxley model (1958) a part of the axon of the cell is modelled as an electrical circuit made up of a capacitor $C$, two (nonlinearly) voltage-dependent conductances $g_{Na}$ and $g_K$ with batteries of voltage $E_{\mathrm{Na}}$ and $E_K$, an ordinary conductance $g_L$ with a battery of voltage $E_L$ and a current-source $I$. The potential-difference between the inside and outside (upper and lower node of the network) of the cell is the membrane potential $V$. The capacitor accounts for the cell membrane and the lipid layer that cover the cell and can take up charge, the voltage-independent conductance for leak-currents that flow in or out of the cell, causing the cell to return to its equilibrium potential $E_L$ if no input current is injected. The voltage-dependent conductances represent the ion channels (in the classical HH-model only sodium and potassium), that open or close at different rates and thereby create the distinct time-course of the membrane potential during a spike. The batteries with $E_K$ and $E_{Na}$ represent the reversal-potential for the specific ion-type. The current-source $I$ represents a current artificially injected into the cell through an electrode or currents flowing into the cell due to synaptic activity.

[3]Nobel Prize in Physiology/Medicine in 1963.

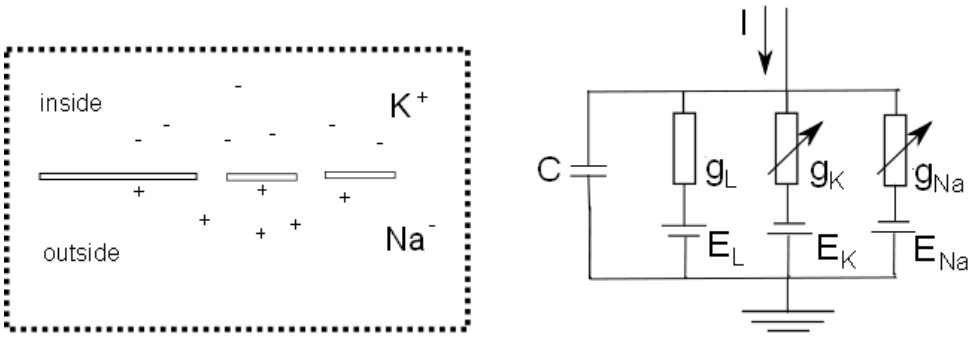


Figure 2: Schematic respresentation of the membrane potential and electrical cirquit used for the Hodgkin Huxley model neuron. Adapted, from [8].

Applying Kirchhoffs Law to the model delivers[4]:

$$C\frac{dV}{dt} = -I_K - I_{Na} - I_L + I(t).$$

The currents are

$$\begin{aligned} I_{Na} &= g_{Na}m^3h(V - E_{Na}) \\ I_K &= g_K n^4(V - E_K) \\ I_L &= g_L(V - E_L). \end{aligned}$$

The dynamics that create the shape of a spike arise from a set of three linear differential equations that determine the behavior of the gating variables $m, h, n$ with voltage-dependent coefficients $\alpha, \beta$ whose voltage-dependence is fitted to experimental measurements.

$$\begin{aligned} \dot{m} &= \alpha_m(V)(1-m) - \beta_m(V)m \\ \dot{n} &= \alpha_n(V)(1-n) - \beta_n(V)n \\ \dot{h} &= \alpha_h(V)(1-h) - \beta_h(V)h. \end{aligned}$$

The model was the first to quantitatively describe the emergence of action potentials and a milestone in the development of biophysics bringing together methods of physics (mainly the modeling and stability analysis of dynamical systems) with biologically relevent questions. In order to analytically study the properties of the system of four differential equations ($V$, $m$, $n$, $h$), simplifications were made by Richard FitzHugh (1955, FitzHugh-Nagumo model) reducing it to a two-variable-system. Many other mathematical neural models exist, building upon the same idea of modeling the membrane potential as a differential equation together with a number of auxiliary variables whose time-dependence is also determined by a differential equation. Examples are the Moris-Lecar model or the Wilson-Lowan model.
This thesis will analyze the behavior of a network of so called "Integrate and Fire" neurons.[5] This neuron model takes advantage of the fact, that action potentials follow a

[4]For details of the HH-moodel see Gerstner & Kistler [8]

[5]This model was already proposed in 1907 by Lapicque but does not explain the mechanisms behind the action potential generation.

stereotypical trajectory, that has not to be accounted for in the equations explicitly. Instead the I&F neuron model only describes subthreshold behavior. Once the membrane potential reaches the threshold $V_{Th}$, a spike with heigth $V_{Sp}$ is inserted into the time-course and the membrane potential is reset to a value $V_{Res}$. The equation of the (leaky[6]) I&F-model can be derived from the Hodgkin-Huxley-Model setting the nonlinear conductances to zero. With the membrane time constant $\tau_m = C\frac{1}{g_L}$ and the membrane resistance $r_m = \frac{1}{g_L}$ this leads to

$$C\frac{dV}{dt} = -g_L(V - E_L) + I(t) \;\Big|\cdot \frac{1}{g_L} \tag{1}$$

$$\Leftrightarrow \boxed{\tau_m \frac{dV}{dt} = -(V - E_L) + r_m I(t)}. \tag{2}$$

This model is computationally more efficient, since it consists only of one differential equation. Therefore it is often used for studies of large artificial networks.
A sometimes useful analogy for this system is a leaky water bucket of a size proportional to $\tau_m$ with a water input stream to output stream-ratio proportional to $\frac{E_L - V}{r_m I(t)}$. If this ratio is larger than one, the bucket will be filled over time (causing it to spill over – the neuron fires a spike), if the ratio is smaller than one, the water level will never reach the brink (never fires a spike). It has to be emphasized, that spikes are not produced by the model itself but have to be inserted in the time course of $V(t)$. This makes the numerical treatment of the differential equation more complicated.
If one records the reaction of a real neuron in vivo for a longer period of time, one will see, that the spiking patterns are hardly ever the same. This is caused by the fact, that a single neuron typically receives synaptic inputs from such a large number of other neurons that exact repetitions of the input-patterns are extremely unlikely. This input is often modeled as stochastic in nature, adding a so-called *noise term* $\sigma\frac{dW}{dt}$ with adjustable strength $\sigma$ to the input current.
The full set of parameters needed for one simulated I&F neuron is:

| | |
|---|---|
| threshold potential | $V_{Th}$ |
| reset potential | $V_{Res}$ |
| spike potential | $V_{Sp}$ |
| equilibrium potential | $E_L$ |
| membrane time constant | $\tau_m$ |
| membrane resistance | $r_m$ |
| input current | $I(t)$ |
| noise | $\sigma$ |

If the spike-timing $t_1, t_2, ...$ of a recording is of importance, then a function called the *neural response function*, consisting of Dirac delta impulses $\delta(t)$ is used.

$$\rho(t) = \sum_i \delta(t - t_i).$$

[6] due to the leak term $-(V - E_L)$

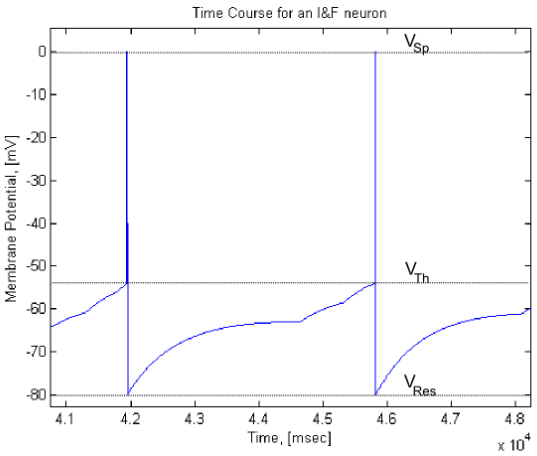


Figure 3: Typical time course of an I&F neuron.

### 2.1.3 Synapses

Synapses connect neurons and have a strong effect on their dynamic behavior. The effect of synapses on their target-neurons can be modeled by defining a synaptic input current $I_S(t) = g_S(t)(V - E_S)$ to the target-neuron, $E_S$ being the characteristic reversal potential for the synapse and $V$ being the membrane potential of the synaptic target. Synapses with $E_S > V_{Th}$ are excitatory, $E_S < V_{Th}$ inhibitory, $V_{Th}$ is the threshold potential for the target neuron. A number of different inhibitory and excitatory synapses are found in the brain, they are classified by the neurotransmitter they use and have different rise and decay times for $g_S(t)$ ranging from less than 1 ms to more than 100 ms. A synapse model explains how $g_S(t)$ evolves over time when spikes described by the neural response function $\sum_i \delta(t - t_i)$ arrive at the synapse. The construction of a realistic synapse-model proceeds in a number of steps starting from detailed kinetics of neurotransmitters that are released at the presynaptic terminal, then cross the synapic cleft and bind to receptors that cause postsynaptic ion-channels to open. The construction of such a model is covered in great detail in [3]. One obtains a differential equation that describes the opening probability or the fraction of open channels $p(t)$ over time and multiplies that with the maximum conductance $\bar{g}_S$ of the synapse in order to get $g_S(t)$. Since the synaptic current to an I&F neuron will be made adjustable with yet another variable, the synaptic strength $w$, the maximum conductance will be lumped together with that strength, the synaptic conductance will normalized to one and the differential equation will be written in terms of $g_S(t)$ instead of $p(t)$.
In this simulation the synaptic conductance with time constant $\tau_S$ evolves according to:

$$\tau_S \frac{dg_S}{dt} = -g_S + \sum_i \delta(t - t_i - \tau_{\text{delay}}).$$

The solution of this differential equation in between spikes is an exponential function $g_S(t) = g_0 exp(\frac{-t}{\tau_S})$. For incoming spikes $g_S(t)$ is being set to $g_S(t) + 1$ after an adjustable synaptic delay of $\tau_{\text{delay}}$. This means, that the synapse is summing inputs linearly. Depression or facilitation – the dependence of conductivity on the history of the synapse – are not modeled.

## 2.2 Dynamical Systems and Bifurcations

In the last chapter it was shown, that an I&F neuron is described by a differential equation. If neurons are connected, those differential equations will be coupled. To analyze their behavior analytically, it is necessary therefore to study systems of differential equations. The branch of mathematics that studies the qualitative behavior of systems described by differential equations is dynamical systems theory. The most important concepts, that will be used in the analysis of the two-neuron-model are explained in this section.

**Dynamical System** A dynamical system is a set of differential equations in $n$ variables with time dependence. It consists of a **state vector** $\vec{x} \in \mathbb{R}^n$ lying in **phase space** and a *smooth* function $F(\vec{x}, t)$ determining the behavior of $\vec{x}(t)$ over time.

$$\dot{\vec{x}} = F(\vec{x}, t)$$

**Fixed Point** A fixed point $\vec{x}_0$ is vector, for which

$$\dot{\vec{x}}_0 = F(\vec{x}_0, t) = 0.$$

Fixed points exhibit differnt types of **stability** – the behavior of the system for small perturbations $\vec{x}_0 + \Delta\vec{x}$ from the fixed point.

**Stability** A fixed point $\vec{x}_0$ of a dynamical system is[7]:

- attractive, if solutions that start close to $\vec{x}_0$ converge to $\vec{x}_0$.
- stable, if solutions that start in the vicinity of $\vec{x}_0$ stay in the vicinity of $\vec{x}_0$.
- asymptotically stable, if it is attractive and stable.
- instable, if not all solutions that start close to $\vec{x}_0$ stay close to $\vec{x}_0$.

**Nullclines** The nullcline for one variable of the dynamical system is the set of points in phase space for which the time derivative of the variable is 0. The intersection of nullclines of a system is a fixed point of the system.

**Periodic Solution** A periodic solution $\vec{x}_p(t)$ is a solution $\dot{\vec{x}}_p(t) = F(\vec{x}_p, t)$ of the system with

$$\vec{x}_p(t + T) = \vec{x}_p(t).$$

A closed trajectory (periodic solution) in phase-space that is not surrounded by other closed trajectories and is therefore isolated is called a **limit cycle**.

**Bifurcation** A bifurcation is a change in the topological structure or number of solutions to the dynamical system as a parameter $\lambda$ is varied. $\lambda$ is the **bifurcation parameter**, the value $\lambda_0$ for which the parameter-dependent system $F(\vec{x}, t, \lambda)$ undergoes a bifurcation if $\lambda > \lambda_0$ is called a **bifurcation point**.

**Hopf Bifurcation** A bifurcation for which a limit cycle that surrounds the fixed point emerges as a solution is called a Hopf[8] bifurcation. For a **subcritical Hopf bifurcation**, the fixed point looses its stability and the system must go into the limit cycle.

[7] [7] p. 34
[8] also Andronov-Hopf

Except for a few special cases dynamical systems can only be traced numerically. Fortunately linear systems $F_L(\lambda_1\vec{x} + \lambda_2\vec{y}) = \lambda_1 F_L(\vec{x}) + \lambda_2 F_L(\vec{y})$ are one of these cases and any system $F(\vec{x}, t)$ can be linearized around a point $\vec{x}_0$ using the first term of a $n$-dimensional Taylor expansion of $F(\vec{x}, t)$, also called the Jacobian of the system. Any linear system can be written as $\dot{\vec{x}} = A(t)\vec{x} + \vec{b}(t), A \in \mathbb{R}^{n\times n}, b \in \mathbb{R}^n$. If the matrix $A$ is independent of time and has a nondegenerate spectrum or for all eigenvalues the algebraic multiplicity $\alpha(\lambda)$ equals geometric multiplicity $\gamma(\lambda)$, the solution of the system can be obtained using an eigenvector-ansatz: $\vec{x}(t) = \sum_{i=1}^{n} c_i exp(\lambda_i t)\vec{v}_i$. The behavior of solutions that start close to fixed points of the system can then be analyzed by determining the eigenvalues $\lambda_i$ of the linear approximation[9]:

- If all eigenvalues $\lambda$ of A have $Re(\lambda) < 0$, the fixed point is asymptotically stable.
- If none of the eigenvalues of A has $Re(\lambda) > 0$ and $\alpha(\lambda) = \gamma(\lambda)$ for all $\lambda$ with $Re(\lambda) = 0$ the fixed point is stable.
- If one of the eigenvalues of A has $Re(\lambda) > 0$ or $\alpha(\lambda) > \gamma(\lambda)$ the fixed point is unstable.
- If $Re(\lambda) = 0$ and $Im(\lambda) \neq 0$, then period solutions exist.

For nonlinear systems the existence of periodic solution is much harder to proof, the Poincaré-Bendixson theorem can be used to show the existence in two-dimensional phase space.

[9] [7] p. 34

## 2.3 Hubel Wiesel Model and Structured Feedback

The visual system is one of the most most intensely studied systems in neuroscience. Models trying to reproduce and explain certain features of the visual system (optical illusions, patterns accuring during migraine or mechanisms behind object recognition) are mostly inspired by the basic physiological architecture of the visual system. While earlier models of the visual system were feed-forward-models, it is known, that feedback[10] is present in the visual system and can therefore have an important role in the encoding-decoding-process of images. In this chapter a short introduction to the physiology of the visual system as well as to the most influential model – the Hubel-Wiesel model – will be given, followed by a presentation of some recent important findings about the detailed structure of this feedback.

Visual signals enter the brain through receptor-cells in the retina in the back of the eye, pass through the optical chiasm, the lateral geniculate nucleus (LGN) – a part of the thalamus – and arrive in the primary visual cortex (V1). V1 is a distinctly functionally structured tissue where these signals are believed to pass through different layers, that extract or integrate features of the stimulus (shape, color, orientation, classification into objects, etc). Neurons in the retina and the LGN show a strong reaction to circular spots of darkness surounded by light or spots of light surrounded by darkness[11]. The first type is termed OFF-center, the second type ON-center cell. Reactions of cells in LGN and V1 depend strongly on the position of the stimuli relative to the eye. The region in which the stimulis ellicits a response is called the receptive field of the neuron. If the stimulus lies outside of that field, the neuron does not react. Neurons in the visual cortex respond strongly to light or dark bars or edges and are divided into two types. For simple cells the reaction depends on the position of these bars, for complex cells it does not. For both kinds of cells the reaction depends on the orientation of the bars. The angle of the stimulus at which they react most strongly, that is with their highest firing rate, is called their *preferred orientation*.

The model proposed by David Hubel and Torsten Wiesel[12] takes some of the mentioned physiological features into account to explain the phenomenon of orientation preference of V1 neurons.

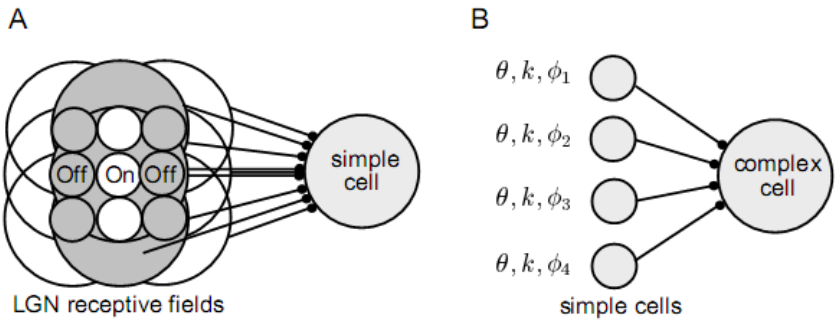


Figure 4: Hubel-Wiesel model of orientation preference in visual cortex. From [6].

[10] Signal propagation from areas that receive synaptic input back to the cells that their input stems from.

[11] Footnote [6] chapter 10.

[12] This model was proposed in 1962, Hubel and Wiesel reveived a Nobel Prize in Physiology/Medicine in 1981.

An array of ON- and OFF-center cells represents the LGN, neglecting the role of retinal cells. Their relative position in the array (see figure 4) also represents their receptive field, indicated by larger circles. They project onto one simple cell in V1 that sums their input linearly. If a bar of light lies along the receptive field of the ON-center neurons, the simple cell receives excitatory input. If the angle of that bar is changed, the OFF-center-cells are also activated, sending inhibitory input to the V1-cell and thereby leading to a decrease in the firing rate of the simple cell. Complex cells are modeled by summing the input of a number of simple cells with same or similar orientation preference but sensitivity in different parts of the receptive field. This Hubel-Wiesel model does not include feedback. It is known though [26], that about about 30% of the synaptic input in LGN stems from V1, while input from the retina only amounts to about 5%. In 2006 Wei Wang et al. [26] experimentally studied the structure of the feedback connections between LGN and V1 cells. A question of particular interest to them was, whether the feedback of V1 (simple) cells influences the ON- and OFF-cells that provide input to them and therefore have the same or similar receptive fields, or if the feedback also goes to cells that do not share the same receptive field. To investigate this, they picked pairs of neurons in LGN and V1 with same receptive fields and measured the effects of feedback indirectly: LGN neurons either fire in tonic or burst[13] mode, and it is known that the ratio between those two modes can be controlled by the strength of cortical feedback. By applying a drug that influences the $GABA_B$-release (neurotransmitter for inhibitory synapses) in V1 they controlled the gain of the cortical cell and studied the effects on the bursting-to-tonic-firing-ratio in the LGN-cell. They found, that the change in this ratio is strongest if the LGN cell has the same receptive fields[14]. These findings led them to suggest an alternative "Reverse Hubel-Wiesel Model" that incorporates the specific structure of the feedback. Figure 5 shows a neuron in V1 (layer 6) that receives feedforward input from one population of ON-center cells and one population of OFF-center cells, both in LGN. While the ON-center cells give excitatory feedforward input to the layer 6 cell, the OFF-center cells give inhibitory feedforward input. The feedback sent from V1 is inhibitory (black dots) for the ON-center cells and projects mainly onto those cells that give feedforward input. The feedback to the OFF-center cells is excitatory and has a similar structure as the feedback given to ON-center cells.
Excitatory feedforward input and inhibitory feedback are termed a "push-pull-relationship" by Wei Wang et al. The fact, that the OFF-center cells receive excitatory feedback and the excitatory ON-center cells receive inhibitory feedback is called "phase reversal".
To study the effects of the structured feedback in a theoretical model, the proposed reverse Hubel-Wiesel model can be implemented using the model neurons and synapses introduced in chapter 2.1.2. There one could simulate how different stimuli can cause the neurons to react. Stimuli that are often used for experiments in the visual cortex are gratings of different orientation and phase as well as isolated bars of darkness or light. There are several ways of "presenting" a stimulus to this theoretical model. The retinal ganglion cells, that translate light intensities into neural spike trains are not part of the model. Instead the intensity of the stimulus will have to directly influence the LGN-cells.

[13] Bursting is a dynamic state where a neuron repeatedly fires discrete groups or bursts of spikes. Each such burst is followed by a period of quiescence before the next burst occurs. (Scholarpedia July 19th 2010, "Bursting") In tonic mode spikes do not arrive in bursts.

[14] But 45% of LGN-cells with different receptive fields than the influenced V1 neuron also showed also a change in their tonic-burst firing ratio.

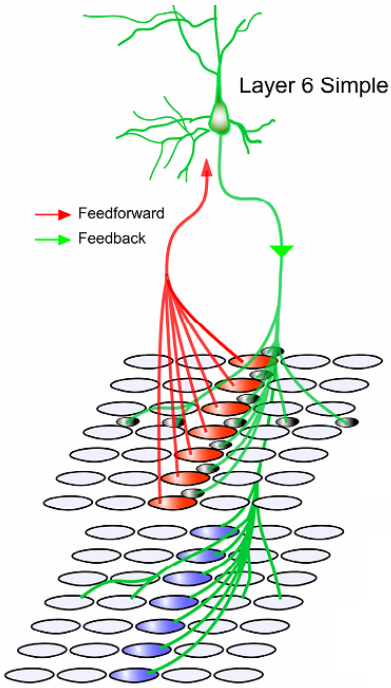


Figure 5: Reverse Hubel-Wiesel model. Black dots indicate inhibitory connections. The two layers are ON and OFF-center cells. From [26].

One way of doing this, is to use a Poisson-process whose rate $r$ has a functional relationship with the stimulus intensity $s$, $r = r(s)$ and create spikes that arrive at synapses of the LGN neurons. But this still leaves open a number of questions – What is the functional relationship $r(s)$ between stimulus intensity and firing rate? What type of synapses should one use? How many synapses? In a more simplified model, an input current of strength $I$, that also has to have a functional relationship with the stimulus intensity is directly injected into the LGN neurons. The stochastic nature of the neural activity is captured by a Gaussian noise current, that is added to the input current as described in chapter 2.1.2.
Now to further simplify the model, instead of looking at a large number of neurons in LGN that project onto the V1 neurons, only one neuron from LGN and one neuron from V1 will be considered. An ON-center neuron from LGN will give excitatory feedforward to V1 and receive inhibitory feedback. This simplification allows to study the parameter combinations for which oscillations emerge in the first place and to experiment with different concepts for the definition of neural codes in a very small, controlled setup.
To see if this model reflects physiological features properly, one would have to find a setup in which it reproduces exeperimentally obtained signals and then check, if for other stimuli it correctly predicts experimental data.

## 2.4 Two Neurons – Spiking Model and Rate Model

The model of two coupled I&F neurons consists of four differential equations – two for membrane-potentials and two for synaptic conductances – and is not analytically tracable, since the firing of spikes and the following reset of the membrane potential is not included in the equations but is crucial to the behavior of the system. According to the definition in chapter 2.2 it is not even a dynamical system, since $F(\vec{x}, t)$ is not a smooth function. Nevertheless some substantial analysis can be carried out if the system is simplified accordingly.
The oscillations of interest are the oscillations of the firing rate. Therefore a mathematical description of the firing rate based on the current model is necessary. The derivation of a firing-rate model can be found in Dayan & Abbott [6] and will be sketched here in order to comment on the choice of some parameters and the synaptic kernel. Questions that have to be answered by the analytical model are:

- For which parameter-combinations do rate-oscillations arise? This can give useful hints to the variation of parameters in the I&F model.
- How does the firing rate of the receiving neuron depend in the input current of the LGN neuron? This is useful for studying the minimum current difference one needs in order to cause a change in the rate detected in a smaller time window.
- How does the feedback-strength influence the oscillations? Oscillations are a necessary reference signal for the phase of firing code.

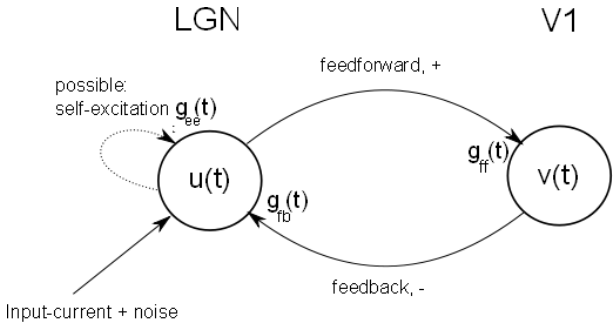


Figure 6: Coupled neurons with input current and noise. $u(t)$ and $v(t)$ can either stand for membrane potentials or firing rates depending on the model used.

The equations describing the system of two coupled I&F neurons including random gaussian noise input are:

$$\tau_{m_U}\frac{dU}{dt} = -(U - E_{L_U}) + g_{\mathrm{fb}} w_{\mathrm{fb}}(U - E_{S_U}) + r_{m_U} I(t) + \sigma\frac{dW}{dt} \tag{3}$$

$$\tau_{m_V}\frac{dV}{dt} = -(V - E_{L_V}) + g_{\mathrm{ff}} w_{\mathrm{ff}}(V - E_{S_V}) \tag{4}$$

$$\tau_{S_{\mathrm{ff}}}\frac{dg_{\mathrm{ff}}}{dt} = -g_{\mathrm{ff}} \tag{5}$$

$$\tau_{S_{\mathrm{fb}}}\frac{dg_{\mathrm{fb}}}{dt} = -g_{\mathrm{fb}}. \tag{6}$$

$w_{\text{fb}}$ and $w_{\text{ff}}$ are parameters to adjust the synaptic strength, the noise-term will not be considered in the following construction of a firing rate model. To construct a firing rate model first the synaptic input to a neuron is written as a function of the firing rate of the neurons projecting onto it. In this case this is only one neuron.

$$I_S(t) = w \int_{-\infty}^{t} d\tau \rho(\tau) K(t-\tau) \tag{7}$$

$\rho(t) = \sum_i \delta(t - t_i)$ is the neural response function of the neuron giving input, $K(t)$ is the synaptic kernel describing the input-current as a function of time in reaction to a single spike. $w$ is the synaptic weight, positive weights are used for excitatory, negative weights for inhibitory synapses. Convoluting the kernel with the neural response function implies, that the the contribution to the input current of each spike sums linearly, which is how the I&F synapse model works. For the synapse model used in the I&F model, ignoring synaptic delays and the dependence of the input current on the current membrane potential V(t)[15], the kernel is $K(t) = exp(-t/\tau_s)/\tau_s$. Now $\rho(t)$ is replaced by $r(t)$, the firing rate of the input-neuron. This is justified, if the spikes in the input-spike train are uncorrelated. When replacing the spike train $\rho(t)$ by a firing rate $r(t)$ the valididy of the synaptic kernel $K(t)$ is in question. At least the time constant $\tau_s$ obtained from the differential equation for the synaptic conductance is not the same and it will therefore be written $\hat{\tau}_s$.
Differentiating $\frac{dI_S(t)}{dt}$ and applying Leibniz' rule for the differentiation of the limits of an integral yields:

$$\frac{dI_S(t)}{dt} = w\, r(t) K(t-t) + w \int_{-\infty}^{t} \frac{\partial}{\partial t} \left[ r(\tau) \frac{exp(-(t-\tau)/\hat{\tau}_s)}{\hat{\tau}_s} \right] d\tau \tag{8}$$

$$\hat{\tau}_s \frac{dI_S(t)}{dt} = w\, r(t) - \underbrace{w \int_{-\infty}^{t} r(\tau) \frac{exp(-(t-\tau)/\hat{\tau}_s)}{\hat{\tau}_s} d\tau}_{=I_S(t)} \tag{9}$$

$$\hat{\tau}_s \frac{dI_S(t)}{dt} = -I_S + w\, r(t). \tag{10}$$

Now the output rate $v(t)$ of a neuron has to be expressed as a function of its synaptic input current, $v(t) = F(I_S)$. For an I&F neuron without absolute refractory period this relationship is approximately given by a threshold linear[16] function $F(I_S) = \alpha[I_S - I_{Th}]_+$ with $\alpha$[17] and $I_{Th}$ being determined by $E_L, V_{res}, V_{Th}, \tau_m, r_m$ of the neuron:

$$\alpha = \frac{r_m}{\tau_m (V_{Th} - V_{Res})} \tag{11}$$

$$I_{Th} = \frac{V_{Th} - E_L}{r_m \tau_m (V_{Th} - V_{Res})} \tag{12}$$

$\alpha$ determines the slope of the input-current firing rate relationship, $I_{Th}$ its offset from zero. The threshold linear function secures two imporant properties of the rate model.

[15] $g_{\text{ff}}(t) w_{\text{ff}} (V - E_{S_V})$, $g_{\text{ff}}(t) w_{\text{ff}} V$ is ignored.
[16] see [6] p. 164
[17] Calculated from the approximate input-firing rate relationship

It first secures that a neuron does not fire ($v(t) = 0$) until its input has exceeded the threshold and secondly prevents the model from producing negative firing rates which don't make physical sense.
Because of the capacitive effects of the membrane (modeled as a capacitor in the I&F model), $v(t)$ does not follow changes of $I_S(t)$ instantaneously. Capacitors in electric ciruits are lowpasses, filtering lower frequencies of the the voltage fluctuation. Therefore an approach using

$$\hat{\tau}_m \frac{dv(t)}{dt} = -v + F(I_S(t)) \tag{13}$$

instead of $v(t) = F(I_S)$ is reasonable. Because $v(t)$ is the firing rate and not the membrane potential, again the membrane time constant $\tau_m$ is replaced by a suitable constant $\hat{\tau}_m$ for the rate model describing how fast the rate can follow changes of $F(I_S(t))$[18].
Now the description of the two cell model still consists of four differential equations, two for the firing rates of the neurons, two for their mutual synaptic input. Exploiting the fact, that the synaptic time constant $\tau_s$ in the I&F model is smaller than the membrane time constant $\tau_m$ and extending this argument to the parameters $\hat{\tau}_s$ and $\hat{\tau}_m$ one can assume that the synaptic current $I_S(t)$ has already settled to its steady state $I_S(t) = w\, v(t)$ while $\frac{dv(t)}{dt}$ is still evolving. Adding the direct input current $I(t)$ to the synaptic input current of the u-neuron this simplifies the rate model to:

$$\hat{\tau}_u \frac{du}{dt} = -u + \alpha_u[-w_{\text{fb}}\, v(t) + I(t) - I_{Th_u}]_+ \tag{14}$$

$$\hat{\tau}_v \frac{dv}{dt} = -v + \alpha_v[w_{\text{ff}}\, u(t) - I_{Th_v}]_+. \tag{15}$$

This system of two ordinary differential equations is now easier to handle than the four equations for the integrate and fire neurons. But a price has to be paid for this simplification: Instead of the precise timing of spikes that can be obtained from the I&F model, the rate model will only give probabilities for spikes. In the course of constructing the rate model several simplifications regarding the synaptic kernel (same for the rate model as for the I&F model ignoring voltage-dependence of synaptic input), the input-firing rate relationship (approximately linear) and the behavior of the input current (settles fast) had to be made. In addition, the actual relationship between the time constants of the rate model and the time constants of the spiking model is not precisely known. Therefore, the analysis of the rate model can give some hints regarding the qualitative behavior of the system. These can simplify the search for a proper setup of the spiking model, but the exact parameters of the spiking model will still have to be found through numerical experiments.

[18] The question of how to reasonably determine the parameters $\hat{\tau}_s$ and $\hat{\tau}_m$ for the rate model from the parameters of the I&F model remains open.

## 2.5 Neural Codes and Information Theory

What would it mean to say that we "understand" the neural code in a particular region of the nervous system? According to Rieke et al. [19] it would mean, that one can – given the spike-trains of a sufficient number of neurons – infer about events that happen in the outside world[19]. Recording for example the response of neurons in the visual cortex of a cat would make it possible for a scientist, who knows the neural code used in visual cortex to tell what the animal has seen. But what exactly is a neural code?
Panzeri et al. [16] define a neural code as:

> "The smallest set of "symbols" capable of representing all information that the neuron carries about the considered stimuli."

This definition builds upon two important concepts:

- The identification of symbols in the context of neuronal recordings. The assignment of spikes or spiking-patterns to symbols depends on the code that is assumed.
- The measurement of information carried by a neuronal recording. Otherwise one could not determine whether "all" information is represented. There has to be a method to determine how much information is contained in a neural recording.

Panzeri et al. [16] identify four properties that are used to characterize different kinds of neural codes:

- The encoding-time-window, which is the temporal window containing the response patterns that are considered as the basic information-carrying units of the code.
- The response-patterns.
- The temporal reference-frame, which is the time axis against which the symbols of the code are measured. This can be defined by external or internal events.
- The temporal precision[20]

The process of decoding, which is what the scientist does when he or she tries to understand neural recordings, is "the extraction of information about the stimulus from a given neural response. For example, predicting the most probable stimulus that could have elicited an observed response"[21]. In analogy to the encoding window that is used by Panzeri et al, a "decoding window" will be used here, which will have the same properties the encoding window has.
In this thesis two types of codes will be considered: a rate code[22] and a phase of firing code[23]. Both codes will be explained briefly and three of the four properties will be defined for the respective code.

[19] [19] p. 16
[20] The temporal precision is defined as the coarsest temporal resolution at which spikes need to be measured without loosing any of the encoded information. This property will not be considered in this thesis.
[21] [16]
[22] abbreviated RC
[23] abbreviated POF code or POFC

### 2.5.1 Rate Code

The rate code builds on the concept of firing rates. Even though the concept is quite simple, "How many spikes are fired per second at an instant?", there is no exact definition of how to assign firing rates to a single neural response $\rho(t)$. Here the definitions given in [6] will be presented.
The neural response function $\rho(t)$ can be averaged over a number of trials, noted $\langle\rho(t)\rangle$. The *firing rate* $r(t)$ is defined as the average sum of spikes fired in a time-interval $\Delta t$ divided by the length of this interval:

$$r(t) = \frac{1}{\Delta t}\int_t^{t+\Delta t} d\tau \,\langle\rho(\tau)\rangle\,.$$

Experimentally this property can be obtained by replacing $\langle\rho(t)\rangle$ by a sum of single neuronal response functions $\langle\rho(t)\rangle \approx \frac{1}{N}\sum_{i=1}^{N}\rho_i(t)$. The approximation of the probability distribution $\langle\rho(\tau)\rangle$ improves as N, the number of trials, is increased.
For a single spike train the firing rate can be obtained by smoothing the spike train with a Gaussian kernel. The firing rate obtained by this process is always dependent on the width of the Gaussian kernel. Another, but also ambiguous measure for a single spike train is the *spike count rate* that depends on the interval $T$:
The *spike count rate* $r$ is obtained by counting all $n$ spikes that occur within an interval $T$ and dividing by the length of that interval: $r = \frac{n}{T}$.

> If a neuron uses a rate code to convey information about its input, its firing rate or spike count rate rather than the precise timing of spikes represents the information.

In the context of the simple two cell model the input will be the current given to the LGN-neuron. The encoding-time-window can have an arbitrary length T, but should not exceed the reaction time of the animal to the specific stimulus. Otherwise it would be hard to claim, that the animal actually "uses" this code to transmit information within the brain. The *symbols* of the code are characterized by the number of spikes occuring within the encoding-time-window which is (apart from the factor $\frac{1}{T}$) the same as the spike count rate. Since it is assumed, that all information is encoded in the the firing rate or spike count rate, no internal or external reference frame is necessary. A possible reference frame could be the onset of the stimulus, though.

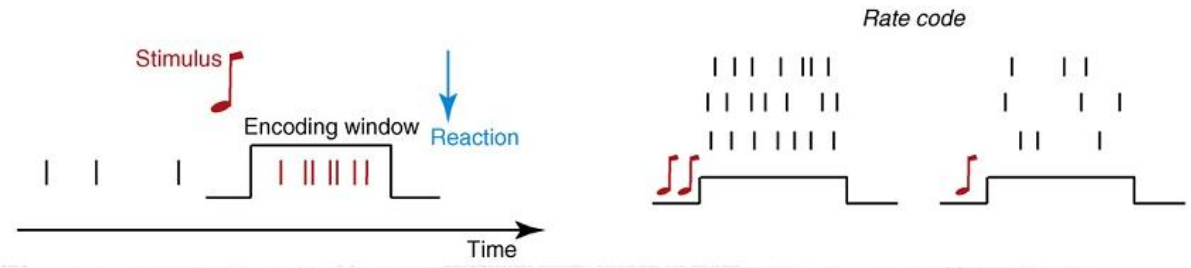


Figure 7: Encoding of stimuli using a rate code. Left – General scheme to explain codes. Right – Rate Code for two differnt stimuli. Taken from [16]

.

### 2.5.2 Phase of Firing Code

Definition:

> A phase of firing code is a code in which stimulus attributes are encoded by the relative timing of spikes to the phase of a network fluctuation.[24]

The network fluctuations can be of different kinds. Montemurro et al. [12] showed, that in rhesus monkeys who were presented with time-varying visual stimuli the timing of spikes in V1 relative to the local field potential (LFP) contained more than 50% additional information about the stimulus. The LFPs are an extracellular signal[25] and are believed to be influenced by some combination of the ionic membrane currents, the membrane potential and the synaptic activity of surrounding neurons. In a theoretical study with a large network (5000 neurons) of randomly connected inhibitory and excitatory I&F neurons Mazzoni et al. [11] created an artificial LFP-signal using weighted synaptic activity of AMPA and GABA synapses. They gave different kinds of input[26] to the network and showed, that this model can encode information about the stimulus in different frequencies of the LFP-fluctuations. They also showed, that the LFP-fluctuations created by the model were similar to those observed in alive monkeys watching a video. A POF code in particular has not been tested by them, they only checked the LFP-fluctuations themselves, not the position of spikes relative to the oscillations of the LFP. This provides another motivation for checking the possibility of a phase code in the two cell model, since this model is the smallest, oscillating component of the larger network they used.
It is often assumed that the reference signal has a sinusodial form $sin(2\pi ft)$ as shown in figure 8, which is also how one would intuitively picture an oscillation. For a phase of firing code the length of the encoding window is then determined by the period-time $T = 1/f$ of one period of the oscillating reference signal. It could also be taken over several periods of the oscillation, but then one had to decide how to assign a single phase tag to several periods.
A POF code can be further divided into phase&rate and phase&pattern code. In this thesis a phase&rate code[27] will be looked at. This determines the possible *symbols* of the code. For a given neural response the spike count within the encoding window is additionally labeled with a phase. This means, that a phase code always contains the information a rate code contains, but has the possibility of adding additional information using the phase label. The general definition of a phase code allows for many possibilities of determining the phase label and two different rules will be checked in chapter 3.4.3.
The definition of a phase of firing code by Panzeri et al. does not commit to the source of the neural reference signal. It can stem from different parts of the brain, like the LFPs in the experiments in rhesus monkeys, as well as from numerical simulations of a model. The challenge in both cases is to identify a reasonable reference signal, that makes obtained spike trains more informative. Extracellular recordings are for example example band pass filtered and only their fluctuations in the gamma band (in Mazzoni's study) considered as a reference signal. The reference signal for the two cell model will have to

[24] [16]
[25] Obtained by electrodes that measure voltage outside of cells.
[26] Constant signal+noise, periodic signal+noise, realistic signal+noise. The realistic signal was obtained from neurons of a monkey watching a video.
[27] For detailed explainations refer to [16].

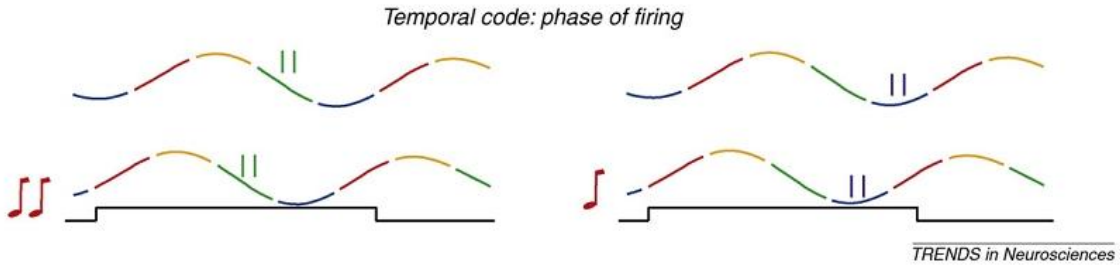


Figure 8: Encoding of two different stimuli using a phase of firing code. Taken from [16].

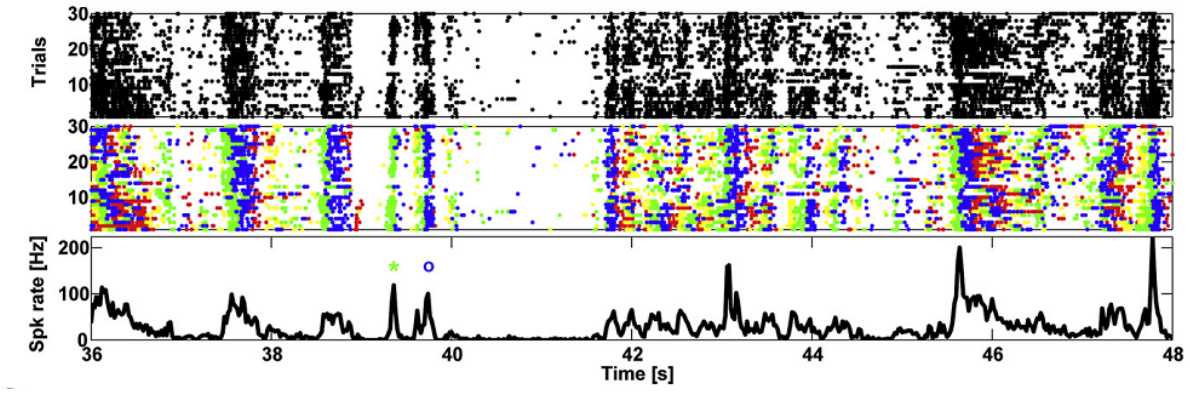


Figure 9: Example for a possible POF code in alive rhesus monkey. The green star and the blue dot indicate reactions at a similar rate to different scenes of a movie. Only when looking at the phase-tagged (colored) spikes in the second row one can distinguish between the scenes. From [12].

| Properties | Rate code | POF code |
|---|---|---|
| encoding-window | arbitrary length, shorter than reaction time | one period of the reference signal or a multiple thereof |
| pattern | spike count in the window | spike count in the window and phase label |
| reference signal | not necessary | to be determined in the simulation, in vivo experiments: LFP |

Table 1: Properties of the RC and POFC.

be defined in more detail in the following chapter 3.4.3. Table 1 gives an overview over the properties for the rate code and phase of firing code.

### 2.5.3 Measuring Information

How much does a neural response tell about the stimulus? This question can be answered quantitatively using information theory. Claude E. Shannon developed information theory in 1948 and 1949 in order to quantitatively assess the abilities of noisy communication channels. The ideas he developed in his seminal paper [21] "A Mathematical Theory of Communication" were originally meant to deal with problems arising in telecommunication, but proved to be very useful for the analysis of neural "communication systems" as well.
According to Shannon's theory a communication channel connects

**A transmitter.** In this case an LGN-neuron, sending spikes to a V1 neuron when stimulied by the input current. In a more general case the transmitter is the whole visual system prior to V1 creating spike trains which depend on the physical properties of the outside world relevant to the system (brightness, contast, edges).

**A receiver.** The upstream neurons in V1, trying to infer information about the current that was injected. In a more general case they are trying to infer the properties of the outside world from the signals they receive from LGN.

that want to communicate

**A message.** In this case a current of intensity I which in this context will also be called the stimulus. In a broader sense possibly facts about the outside world (eg. "blue truck approaching at high speed from the right").

By means of a

**A signal.** The spike trains exchanged between LGN and V1 neurons.

But the communication is complicated by

**A noise source.** In this case the background-activity of other neurons in the network whose activity is uncorrelated with the stimulus properties, but whose activity influences the LGN and V1 neuron.

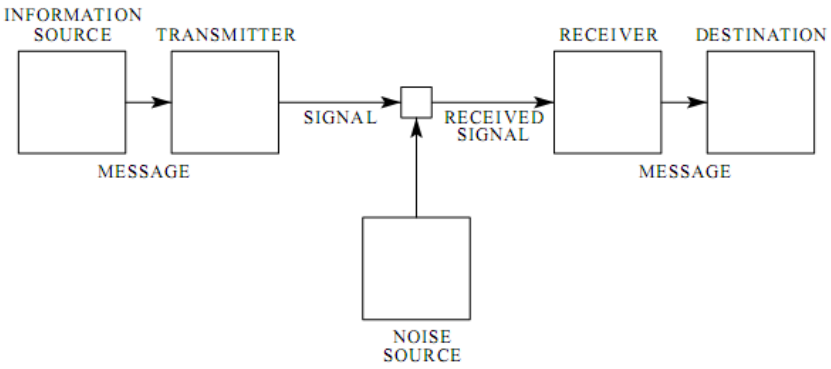


Figure 10: Communication channel according to Shannon. Information source and destination are not mentioned here. From [21].

The fundamental quantity of information theory is the entropy. The same way in which physical laws limit for example the resolution of optical instruments[28], the entropy of a communication channel limits its ability to transmit information. The entropy $H$ is defined[29] as

$$H = -\sum_r P[r] log_2 P[r].$$

P[r] denotes the probability of receiving the symbol "r". These "r" are drawn from a known set, the alphabet of the code, and are the symbols used by the code as explained in the previous chapter.
While the entropy $H$ measures the maximum capacity of a communication channel, the mutual information $I_M$ measures how much of this capacity can be used due to noise impairing the transmission. A number of probabilites have to be introduced to calculate the mutual information:

- P[s] – probability of a stimulus being presented (prior probability)
- P[r] – probability for a certain symbol of the code to occur
- P[r, s] – probability of stimulus s being presented and response r being recorded (joint probability)
- P[r|s] – probability of evoking response r, given the stimulus s (conditional probability). Response and symbol are sometimes used interchangeably since the symbols can be created from the resonse if the necessary rules are given.
- P[s|r] – probability that stimulus s was shown, given the response r

If only one stimulus is presented over a number of trials, the received symbol will not always be the same because of the noise. The entropy $H_S$ for one stimulus $s$ and the different received symbols $r$ is:

$$H_S = -\sum_r P[r|s] log_2 P[r|s].$$

[28] [19]
[29] for a motivation see for example Dayan&Abbott [6] p. 124

Using this quantity the noise entropy $H_{Noise}$ is defined as

$$H_{Noise} = \sum_s P[s]H_S = -\sum_s \sum_r P[s]P[r|s]log_2 P[r|s].$$

The mutual information $I_M$ is defined as $I_M = H - H_{Noise}$ which can be simplified to

$$I_M = \sum_s \sum_r P[r|s]P[s]log_2(\frac{P[r|s]}{P[r]}).$$

The maximum value for the mutual information is the entropy of the sender, $H$. For equal probabilities of stimuli $P[s_1] = P[s_2] = ... = P[s]$ this is $I_{M_{\max}} = -log_2(P[s])$. For two possible symbols, $I_{M\max} = 1$ bit.[30] This fact can for example be used to test if the implementation of the `CalculateIM` routine (see appendix) in MATLAB is correct.
If for the same set of stimuli one communication channel has a higher mutual information than another channel, this means, that if one receives a symbol "r", one is more confident, that a particular message was sent.

[30] The unit of the entropy depends on the base of the logrithm that is used. For a base 2 logarithm it is 1 bit.

# 3 Two Cell Model

Now the tools for analyzing the information transmission ability of the two cell model of thalamocortex have been introduced. After a setup has been found for the spiking model that can cause the system to oscillate, rate and phase of firing code will be used to encode and decode the input current given to the system. In order to find that setup and to get some understanding about how oscillations emerge, first a bifurcation analysis will be carried out on the rate model. This will give hints to the choice of the membrane time constants and feedback strengths and will also allow prediction of the frequency of firing rate oscillations depending on the input current and the feedback strength.

## 3.1 Analytical Investigation of the Rate Model

The analytical model describing the firing rate of the system of the two coupled I&F neurons is[31]:

$$\hat{\tau}_u \frac{du}{dt} = -u + \alpha_u[-w_{\text{fb}}\, v(t) + I(t) - I_{Th_u}]_+ \tag{16}$$

$$\hat{\tau}_v \frac{dv}{dt} = -v + \alpha_v[w_{\text{ff}}\, u(t) - I_{Th_v}]_+. \tag{17}$$

This system is nonlinear due to the threshold. The threshold-terms are turned on and influence the system for $I(t) > w_{\text{fb}} v(t) + I_{\text{Th}_u}$ (criterion 1) and $u(t) > \frac{I_{Th_v}}{w_{ff}}$ (criterion 2). If both criteria are *not* met, then the system can be written as

$$\frac{d}{dt}\begin{pmatrix} u \\ v \end{pmatrix} = \begin{pmatrix} -1/\tau_u & 0 \\ 0 & -1/\tau_v \end{pmatrix}\begin{pmatrix} u \\ v \end{pmatrix}. \tag{18}$$

This case corresponds to an input-current $I(t)$ that lies below threshold $I_{Th_u}$ with initial values $u_0, v_0$ that also do not satisfy the two criteria. This system has only one fixed point at $(0,0)$. A linearization around that point is not necessary since the system is already linear. The eigenvalues can be directly determined from the diagonal of the matrix and are obviously real and negative. Therefore no oscillations will occur, but the system will return to the fixed point $(0,0)$ if perturbed from it. Because of the linearity of the system this holds for perturbations of arbitrary strength as long as they lie within the scope of equation 18.
If both criteria are met – the input-current is above the threshold and $u(t), v(t)$ are in a region of phase space where they fulfill the inequalities – the system takes the form

$$\frac{d}{dt}\begin{pmatrix} u \\ v \end{pmatrix} = \begin{pmatrix} -1/\tau_u & -\alpha_u w_{fb}/\tau_u \\ \alpha_v w_{ff}/\tau_v & -1/\tau_v \end{pmatrix}\begin{pmatrix} u \\ v \end{pmatrix} - \begin{pmatrix} [I_{Th_u} - I(t)]\alpha_u/\tau_u \\ I_{Th_v}\alpha_v/\tau_v \end{pmatrix}. \tag{19}$$

This is a system of the type $\dot{\vec{x}} = A\vec{x} - e^{\mu t}\vec{b}$ with $\mu = 0$ for which an algebraic solution exists. The solution for the homogenous system $\dot{\vec{x}}_H = A\vec{x}_H$ can be obtained using an eigenvector ansatz, the solution for the inhomogeneous system can be found using an ansatz $\vec{x}_P = e^{\mu t}\vec{h}$ to obtain the coefficients of $\vec{h}$. The full solution is $\vec{x} = \vec{x}_H + \vec{x}_P$, the initial conditions are satisfied by the coefficients of the eigenvector ansatz. The dynamical

[31] The choice of this model and parts of the bifurcation analysis were inspired by [6] p. 266, the calculations were performed independently.

behavior for perturbations that stay within the validity of the dynamical system (conditions 1&2) is only determined by the eigenvalues of $A$, the inhomogeneity has no effect on the eigenvalues, but on the position of the fixed point of the system. The fixed point at $\vec{x}_0 = e^{\mu t} A^{-1} \vec{b}$. The inhomogenity in the equation causes the fixed point (0,0) to vanish. The phase portraits can be found in table 4. The eigenvalues of $A$ are:

$$\lambda_{1,2} = -\frac{\tau_u + \tau_v \pm \sqrt{(\tau_u + \tau_v)^2 - 4\tau_u\tau_v\,(w_{\mathrm{fb}} w_{\mathrm{ff}} \alpha_u \alpha_v + 1)}}{2\tau_u\tau_v} \tag{20}$$

The fixed point looses its stability if one of the eigenvalues $\lambda_{1,2}$ is greater than 0. The system starts to oscillate, if the the imaginary part of the eigenvalues is nonzero. A total of 6 parameters can be varied in order to change real and imaginary part of the eigenvalues. The effects of $w_{\mathrm{ff}}, w_{\mathrm{fb}}, \alpha_u, \alpha_v$ are multiplied in the square root, therefore it is only their relative proportions that are of importance and setting $\alpha_u = \alpha_v = 1$ reduces the number of parameters to 4. The fixed point $\vec{x}_0$ for this case lies at

$$\vec{x}_0 = \frac{1}{w_{\mathrm{fb}} + w_{\mathrm{ff}}} \begin{pmatrix} w_{\mathrm{fb}} I_{\mathrm{Th}_v} + I(t) - I_{\mathrm{Th}_u} \\ w_{\mathrm{ff}} I(t) - w_{\mathrm{ff}} I_{\mathrm{Th}_u} - I_{\mathrm{Th}_v} \end{pmatrix}. \tag{21}$$

Notice how the position of this point depends on the current $I(t)$ injected into the u-cell. The stronger the input current, the higher the rates at which the system settles to its fixed point. Not surprisingly the feedforward strength $w_{\mathrm{ff}}$ modulates this position for the v-neuron.
Now three cases will be investigated:

- $w_{\mathrm{ff}} = 1, w_{\mathrm{fb}} = 0$ – only feedforward connections
- $w_{\mathrm{ff}} = w_{\mathrm{fb}} = 1$ – equally strong feedforward and feedback
- $10 w_{\mathrm{ff}} = w_{\mathrm{fb}} = 10$ – very strong feedback

The time constant of the u-neuron is chosen $\tau_u = 1$ for all cases, $\tau_v$ is varied. The dependence of the real and imaginary part and therefore the stability of the fixed point on the value of $\tau_v$ is plotted in the diagrams on page 31.
The diagrams show that for none of the parameter combinations the fixed point will ever loose its stability ($Re(\lambda) > 0$). This seems plausible, since there is no self-coupling included in the model. Therefore there is no force that will keep the rates going up, except for the constant input current. One can see, that the return trajectory to the fixed point is influenced by $\tau_v$. The higher $\tau_v$ is chosen, the slower the system will return to its fixed point because $Re(\lambda)$ is smaller. The return trajectory will either be a direct line or a spiral, depending on the imaginary part of the eigenvalues. For the case without feedback the return will be direct, while for the feedback-cases the state of the system will spiral back into the fixed point. Models without self-feedback of the cells can obviously not show *sustained* oscillations. Therefore self-excitation has to be added to the model!
The equation for the u-neuron changed to:

$$\hat{\tau}_u \frac{du}{dt} = -u + \alpha_u[-w_{fb}\, v(t) + w_{ee} u(t) + I(t) - I_{Th_u}]_+ \tag{22}$$

$w_{\mathrm{ee}}$ is the strength of self-coupling of the neuron. The phase-portrait changes, the slope of the u-nullcline becomes positive. The flow directions are indicated in the right figure

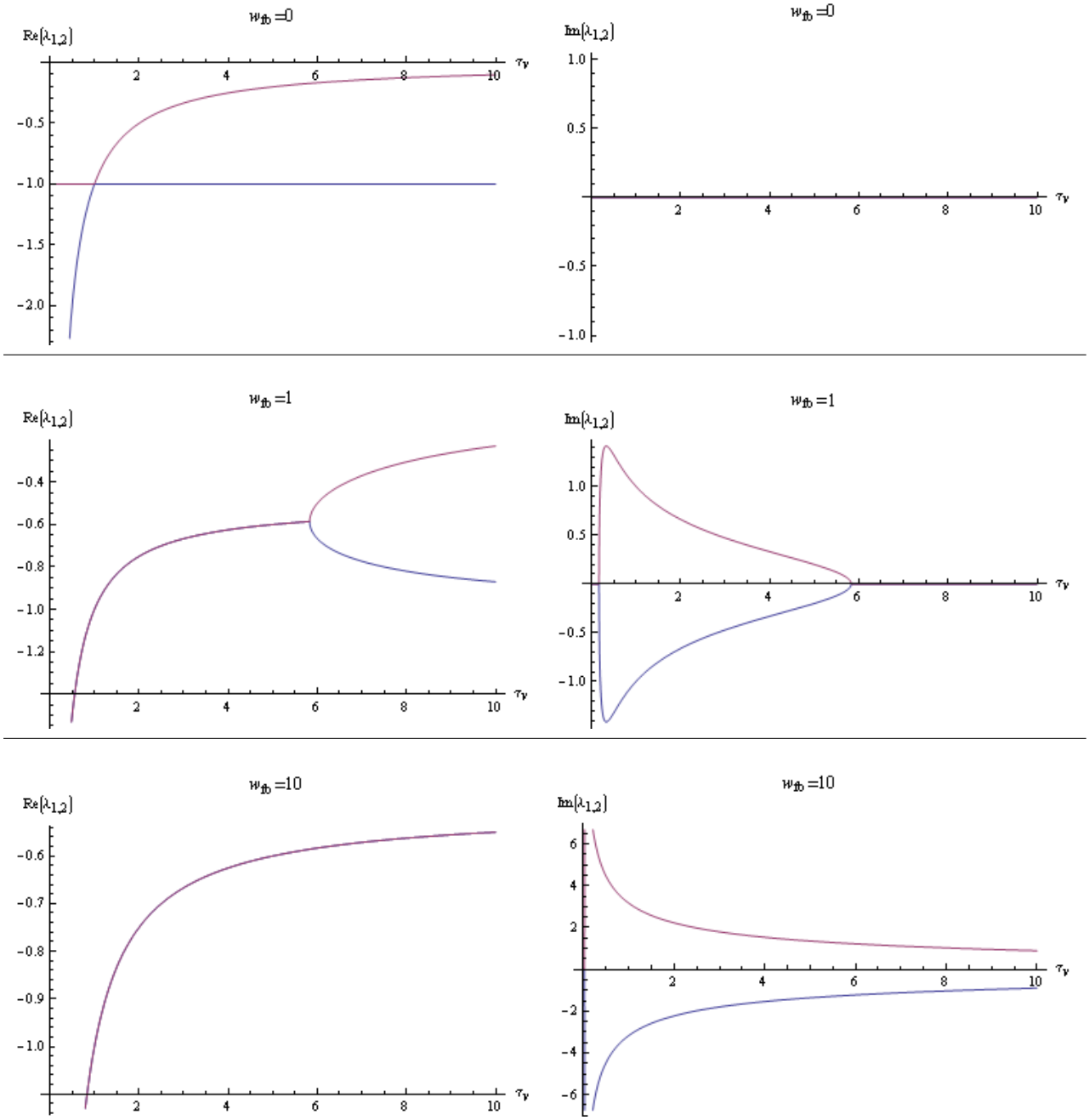


Table 2: Real and imaginary part of the eigenvalues of A as a function of $\tau_v$ for the system without self-excitation. Notice how the $Re(\lambda)$ never crosses 0.

in table 5. The fixed point now lies at

$$\vec{x}_0 = \frac{1}{1 - w_{\mathrm{ee}} + w_{\mathrm{fb}} w_{\mathrm{ff}}} \begin{pmatrix} w_{\mathrm{fb}} I_{\mathrm{Th}_v} + I(t) - I_{\mathrm{Th}_u} \\ w_{\mathrm{ff}} I(t) - w_{\mathrm{ff}} I_{\mathrm{Th}_u} - I_{\mathrm{Th}_v}(1 - w_{\mathrm{ee}}) \end{pmatrix}. \tag{23}$$

The system in the domain where both threshold terms are activated is:

$$\frac{d}{dt}\begin{pmatrix} u \\ v \end{pmatrix} = \begin{pmatrix} (w_{ee}\alpha_u - 1)/\tau_u & -\alpha_u w_{\mathrm{fb}}/\tau_u \\ \alpha_v w_{\mathrm{ff}}/\tau_v & -1/\tau_v \end{pmatrix} \begin{pmatrix} u \\ v \end{pmatrix} - \begin{pmatrix} [I_{Th_u} - I(t)]\alpha_u/\tau_u \\ I_{Th_v}\alpha_v/\tau_v \end{pmatrix}. \tag{24}$$

The eigenvalues are:

$$\lambda_{1,2} = -\frac{\tau_u + \tau_v(1 - w_{\mathrm{ee}}\alpha_u) \pm \sqrt{4\left(-1 + w_{\mathrm{ee}}\alpha_u - w_{\mathrm{fb}} w_{\mathrm{ff}} \alpha_u \alpha_v\right)\tau_u\tau_v + \left(\tau_u + (1 - w_{\mathrm{ee}}\alpha_u)\,\tau_v\right)^2}}{2\tau_u\tau_v} \tag{25}$$

$\alpha_u = \alpha_v = 1$, $w_{\mathrm{ff}} = 1$ and $\tau_u = 1$ are chosen again. Particular attention has to be paid now to the excitatory self-feedback $w_{ee}$ and its influence on the bifurcation point of $\tau_v$. For $w_{ee} < 1$ no instability ever occurs since it can be shown that both eigenvalues are smaller than 0: Because of the negative sign in front of the fraction it only has to be shown that the numerator is always larger than 0. This leads to an inequality $1+\tau_v(1-w_{\mathrm{ee}}) \pm \sqrt{\ldots} > 0$. $1+\tau_v(1-w_{\mathrm{ee}}) > 0$ is true for all physical relevant (positive) $\tau_v$ if $w_{\mathrm{ee}} < 1$, adding $\sqrt{\ldots}$ does not change that. To show that subtracting the root will also leave the nominator above 0 only requires to solve another inequality $1 + \tau_v(1 - w_{\mathrm{ee}}) > \sqrt{\ldots}$ that can be verified by squaring both sides.
For $1 < w_{ee} < 2$ the bifurcation point of $\tau_v$ lies above the value of $\tau_u = 1$ and approaches $\tau_u$ as $w_{ee}$ is increased.[32] If $w_{ee} > 2$ one eigenvalue $\lambda$ has $Re(\lambda) \geq 0$ for all values of $\tau_v > 1$ and therefore the fixed point is not stable. This can be shown again by looking at the nominator of equation 25 which now has to be smaller than 0: $1 + \tau_v(1 - w_{\mathrm{ee}}) \pm \sqrt{\ldots} < 0$. $1 + \tau_v(1 - w_{\mathrm{ee}}) < 0$ for any $\tau_v > 1$ if $w_{\mathrm{ee}} > 2$. Subtracting the root makes it even more negative (or adds an imaginary part to the eigenvalue).
Now the influence of the feedback-strength for $w_{ee} = 1.5$ is studied using the same combination of feedforward and feedback strengths used for the model without self-excitation. The formula for the eigenvalues simplifies to

$$\lambda_{1,2} = \frac{0.5\tau_v - 1 + \pm 0.5\sqrt{4 + 4\tau_v - 16 w_{\mathrm{fb}}\tau_v + \tau_v^2}}{2\tau_v} \tag{26}$$

If no feedback is present $w_{fb} = 0$, the system is unstable for every $\tau_v$. The imaginary part of the eigenvalues $Im(\lambda_{1,2}) \equiv 0$, therefore no oscillations will occur. If the system is perturbed slightly $\vec{x}_0 + \Delta\vec{x}$ in a direction $\Delta\vec{x}$ with $\Delta\vec{x} \cdot \vec{v}_1 \neq 0$ ($\vec{v}_1$ being the eigenvector to the eigenvalue with $Re(\lambda_1) > 0$) the perturbation will increase exponentially, that means that the firing rate will "blow up".
In the presence of feedback over a certain threshold, which is determined by the strength of self-excitation, the system shows a region of stability $Re(\lambda_{1,2}) < 0$ for $\tau_v < 2\tau_u$. The position of the bifurcation point does not depend on the strength of the feedback, whether it is strong or weak, it always lies at $\tau_v = 2\tau_u$. But comparing $Im(\lambda_{1,2})$ at $\tau_v = 2$ for $w_{fb} = 1$ and $w_{fb} = 10$ shows that the frequency of oscillation, $\mathrm{I}m(\lambda)$, depends on the

[32] These results can be reproduced using the Mathematica scripts in the appendix.

strength of feedback. The feedback also influences the position of the fixed point and the intersection of the nullclines with the axes. Taking a look at equality 23 reveals, that the v-coordinate of the fixed point will decrease if the feedback is increased. The intersection of the nullclines with the axes also moves closer towards the origin as $w_{\text{fb}}$ goes up. Therefore stronger feedback will lead to a higher oscillation *frequency* of the rates, but the v-rate itself will decrease.
Having introduced the self-excitation, there are now two ways for the system to show self-sustained oscillations. One way is choosing $\tau_v$ so, that the real part of the eigenvalues vanishes. All perturbations from the fixed point will then neither increase nor decrease with time, but the system will circle around the fixed point forever. This is a periodic solution, but not a limit cycle according to the definition on page 14, since the system now has infinitely many such periodic solutions, but they are not isolated. $\tau_v$ has to be set to the exact value $\tau_v = 2\tau_u$, otherwise the system will always either return to the fixed point or drift away.
This drifting away, which occurs for all $\tau_v > 2\tau_u$, however is turned into a real limit cycle by the rectifying nonlinearity. If the fixed point becomes unstable and the system is slightly perturbed from it, the behavior of the system is determined by the flow field in phase space. One can see from the flow lines in table 5, that the solutions that start close to the fixed point get carried out towards the axes. Because of the nonlinear rectification, the trajectories cannot cross these axes, move towards the origin and are carried out again. This is a periodic solution, since if the system leaves leaves the u-axis after the point at which the v-nullcline hits the u-axis, it will always be carried back to the v-axis, down to the u-axis and so forth. Since the system $A$ itself does not depend explicitly on time if the stimulus is held constant, the trajectories will hit and leave the axes at the same point for every cycle, so that this is a real periodic solution. Because the fixed point lost its stability and a limit cycle occured during the bifurcation, this is a subcritical Hopf bifurcation. The duration of the limit cycle might be calculated analytically, if broken up into three parts (u-axis, v-axis and circeling out over 90 degrees) and integrated seperately. Thereby the frequency of the rate oscillation could be determined.
Quantitative implications of the subcritical Hopf bifurcation for the oscillation frequency of the I&F model are hard to draw. One thing it suggests, is that there is a setup for the I&F model for which the firing rates oscillate contineously without an oscillating input current. These are the rough guidelines for the setup of the spiking model obtained from the rate model:

- The system needs self-excitation, otherwise it cannot show self-sustained oscillations using either an elliptic periodic solution ($Re(\lambda_{1,2}) = 0$) or the limit cycle emerging through a Hopf bifurcation. Without self-excitation it will never become unstable for any changes of $\tau_v$ or $w_{\text{fb}}$. If perturbed, it would oscillate, but would eventually always go back to its fixed point.

- Negative feedback is necessary, otherwise no oscillations of the firing rate will occur. It also prevents the firing rate from blowing up when self-excitation is used.

- The frequency of the rate-oscillation is determined by the strength of the feedback, the stronger the feedback the higher the frequency. The bifurcation point of $\tau_v$ is not influenced by the feedback.

- The time-constant $\tau_v$ of the inhibited v-neuron has to be larger than the one for the excited u-neuron $\tau_u$ in order to cause an oscillation.

Risks of a blow-up of the firing rates are:

- Self-excitation $w_{\text{ee}}$ is chosen to high or feedback is not high enough.
- Time constant of the v-neuron, $\tau_v$ is too high relative to $\tau_u$

Wolfram Mathematica proved to be a valuable tool for exploring the stability of dynamic systems. Scripts that were used to explore the self-excitatory system are included in the appendix. Particularly useful is the `Manipulate` function. For bifurcation analyses of more complex systems `XPPAUT` is a very powerful tool.
A final comment should be given to the time-dependence of a perturbation and the following bifurcation of the system, a fact that is not always covered in the literature. When using the eigenvector ansatz for the solution of the Jacobian of the system, one assumes that the parameters of the system – including the bifurcation parameter – do not change over time. Otherwise such an ansatz would not be possible, integral bases would have to be used instead[33] Therefore a bifurcation occurs only for a system that is restarted from initial conditions every time the bifurcation parameter is varied. The same holds true for the position of the fixed point in phase space – the bifurcation analysis given here can not determine how the system would "follow" a fixed point that moves over time due to the change of some parameter. Especially changes of the rates following $I(t)$ would be interesting!

[33] See for example Heuser [10].

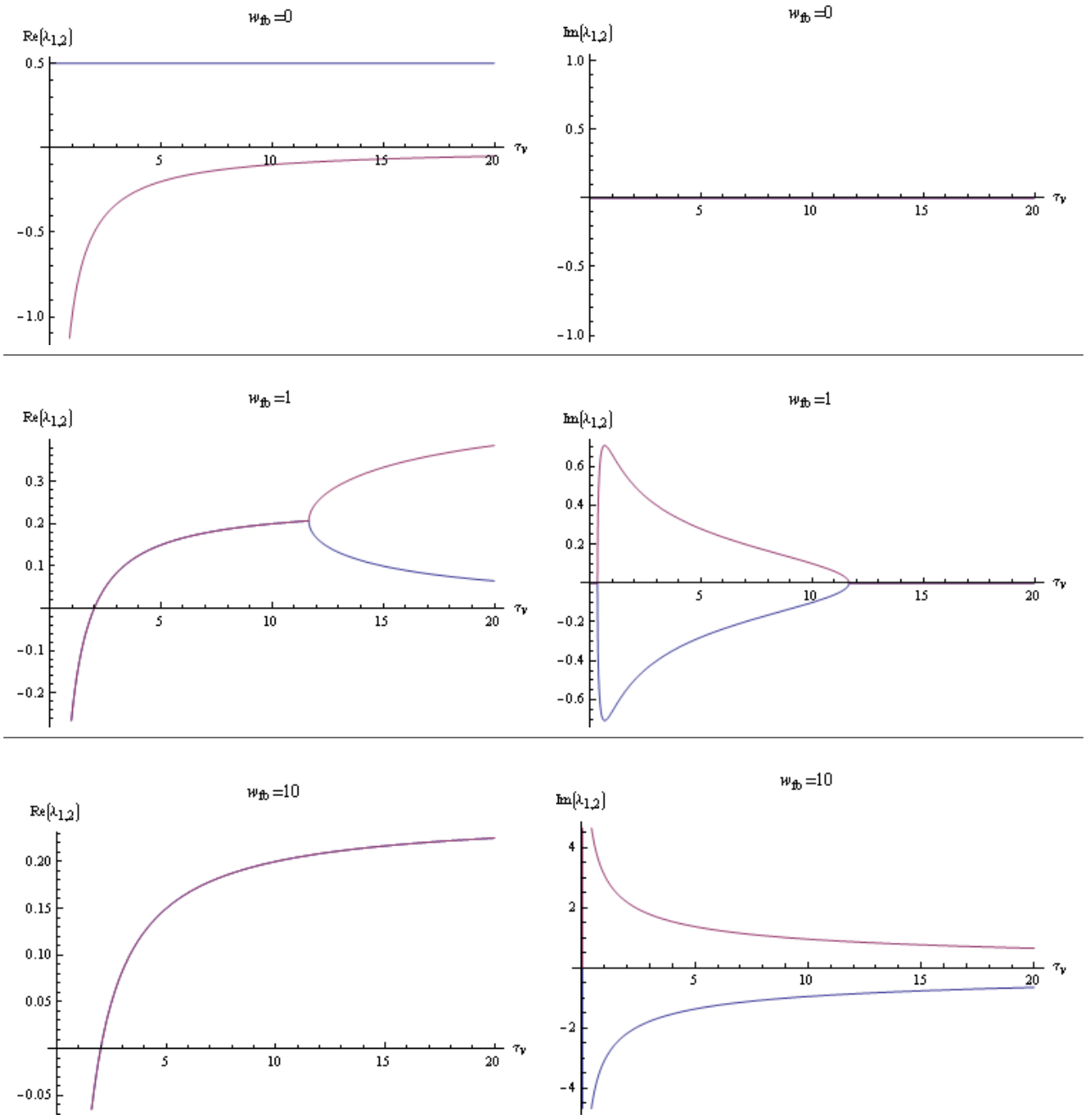


Table 3: Real and imaginary part of the eigenvalues of A as a function of $\tau_v$ for the system with self-excitation $w_{ee} = 1.5$.

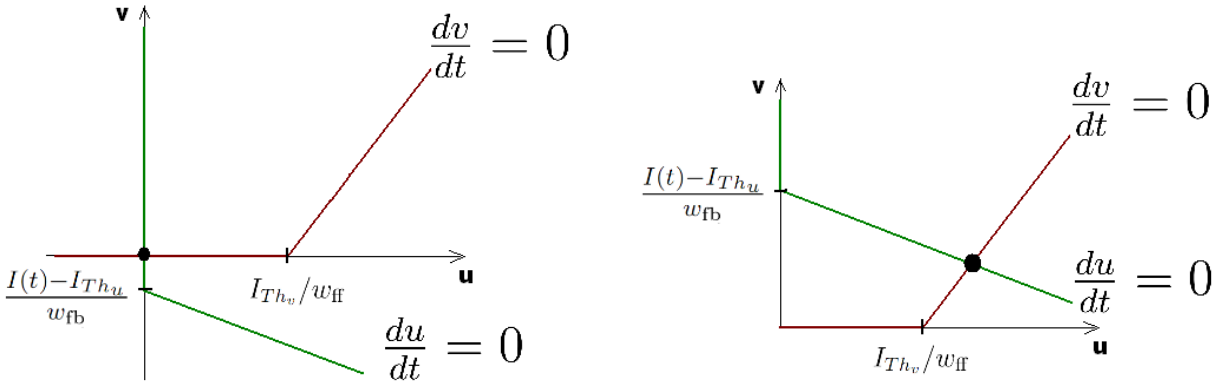


Table 4: Nullclines and fixed point of the system without self-excitation. Left – $I(t) < I_{Th_u}$. Right – $I(t) > I_{Th_u}$.

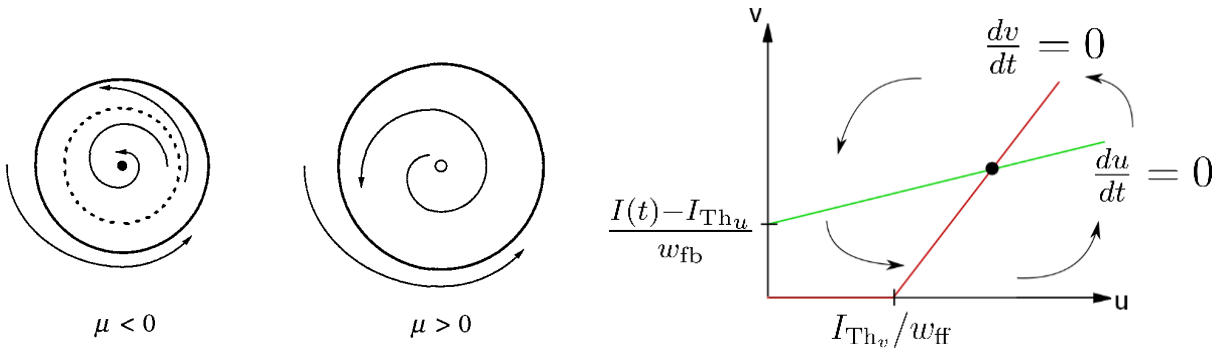


Table 5: Left – Subcritical Hopf bifurcation. $\mu$ is the bifurcation parameter. Filled dots indicate stable, dots with a white center instable fixed points. The closed circle indicates a limit cycle and corresponds to the effects of the rectifying nonlinearity. From Strogatz [23] p. 252. Right – Nullclines and flowfield for the system with self-excitation for $I(t) > I_{Th_u}$ making a subcritical Hopf bifurcation possible.

## 3.2 Numerical Simulation of the Spiking Model

### 3.2.1 Numerical Methods and Parameters

The equation describing the I&F neurons and synapses in the simple feedback-loop, now with self-excitation $g_{\mathrm{ee}} w_{\mathrm{ee}}(U - E_{S_U})$ [34] are:

$$\tau_{m_U} \frac{dU}{dt} = -(U - E_{L_U}) - (g_{\mathrm{fb}} w_{\mathrm{fb}} - g_{\mathrm{ee}} w_{\mathrm{ee}})(U - E_{S_U}) + r_{m_U} I(t) + \sigma \frac{dW}{dt} \quad (27)$$

$$\tau_{m_V} \frac{dV}{dt} = -(V - E_{L_V}) - g_{\mathrm{ff}} w_{\mathrm{ff}} (V - E_{S_V}) \quad (28)$$

$$\tau_{S_{\mathrm{ff}}} \frac{dg_{\mathrm{ff}}}{dt} = -g_{\mathrm{ff}} + \sum_i \delta_U(t - t_i) \quad (29)$$

$$\tau_{S_{\mathrm{fb}}} \frac{dg_{\mathrm{fb}}}{dt} = -g_{\mathrm{fb}} + \sum_i \delta_V(t - t_i) \quad (30)$$

$$\tau_{S_{\mathrm{ee}}} \frac{dg_{\mathrm{ee}}}{dt} = -g_{\mathrm{ee}} + \sum_i \delta_U(t - t_i). \quad (31)$$

$\delta_U(t)$ and $\delta_V(t)$ are the spikes fired by the respective neurons. The system of the two synaptically coupled I&F neurons without the noise term is described by five ordinary, first-order differential equations. This poses an initial value problem. These equations can readily be integrated and MATLAB's `odeXX` routines would be the first choice, the only input they need are the initial values and the right hand side of the differential equations. The reset of the membrane potential for $U(t)$ and $V(t)$ can either be seen a restart of the integration with old initial values or as a discontinuous right side of the differential equations that comes into effect for $V > V_{\mathrm{Th}}$. Resetting the membrane potential $V(t)$ to $V_{\mathrm{Res}}$ is basically a downward step in the membrane potential, that for example in control theory is described by the Heaviside-function. The derivative and therefore an appropriate right side for the differential equation would be the Dirac $\delta$ function.
The two most widely used methods for integrating ordinary differential equations are the Euler and the Runge-Kutta method. While the Euler method for ordinary differential equations requires only one evaluation of the right side, the fourth order Runge-Kutta method requires four evaluations of the kind[35]

$$\begin{aligned} k_1 &= \Delta t f(t_n, V_n) \\ k_2 &= \Delta t f(t_n + 1/2h, V_n + 1/2k_1) \\ k_3 &= \Delta t f(t_n + 1/2h, V_n + k_3) \\ k_4 &= \Delta t f(t_n + h, V_n + k_4). \end{aligned}$$

$f(t, V)$ stands for the right hand side of the differential equations, $\delta t$ for the time step of the numerical method. It is conceptually difficult to handle, if for example $V_n + 1/2k_1 < V_{Th}$ and the regular right side of can be evaluated, but $V_n + 1/2k_2 > V_{Th}$ and the evaluation

[34] This model differs from the standard-way of implementing self-excitation. Using a $g_{\mathrm{ee}} w_{\mathrm{ee}}(U - E_{S_U})$ term to incorporate self-excitation increases the current that is injected into the u-neuron as its voltage U approaches the firing threshold. Please refer to the first page of this thesis (Note Added in Proof).

[35] [17]

of the right side would yield $-\infty$ (the value of the $\delta$ function that creates a downward step). Therefore the Euler method will be applied instead, because this method makes it easier to determine if in the next time step a spike should be fired or not.
A comparison of different numerical methods for integrate and fire neurons can be found in the work by Hansel et al. [9]. Effects of those numerical methods on network-synchronization are also studied there. These effects include the deviance of spike timing, average firing rates and overall network synchrony[36]. Since network synchrony, although in a very small network, in the form of oscillations of the firing rate will be used to encode information, different numerical integration-schemes can cause different results. Hansel's results suggest the use of a second order Ruge-Kutta method with interpolation of spike times that is numerically cheaper then the Euler integration since much larger step sizes are allowed for the same relative error. Nevertheless sufficiently small time-steps ($\Delta t = 10^{-3} ms$ for the standard Euler) lead to the same results and all methods converge towards the exact solution with decreasing time step. Since the model considered here is comparatively small ($\ll 100$ neurons) using an Euler algorithm is acceptable in terms of computational time.
Apart from the spikes, another problem is the $\sigma \frac{dW}{dt}$ term that turns the ordinary into a stochastic differential equation. This makes the application of the built-in MATLAB `odeXX` functions impossible. Instead an Euler-Maruyama method Eulers contribution to this method is the approximation of the solution of an ordinary differential equation by replacing the derivative of a function $\frac{dV(t)}{dt}$. It can be motivated using a first order Talor approximation of $V(t + \Delta t)$. $V(t + \Delta t) = V(t) + \frac{dV(t)}{dt}|_t \Delta t + \mathcal{O}(\Delta t^2)$ yielding

$$\frac{dV}{dt} = \frac{V(t + \Delta t) - V(t)}{\Delta t} + \mathcal{O}(\Delta t). \tag{32}$$

Maruyama added the discretization of the Wiener process $dW(\mu = 0, \sigma^2)$, that can be intuitively understood picturing a Normal distribution $N(\mu = 0, \sigma^2 \Delta t)$ with a variance $\sigma^2 \Delta t$ that grows linearly with the length of the time-step and normalizing this distribution to $\sigma \sqrt{\Delta t} N(\mu = 0, 1)$.
The numerical evaluation scheme is therefore:

$$\boxed{V(t + \Delta t) = V(t) + \Delta t \left[-g_L(V - E_L) + r_m I(t)\right] + \sigma \sqrt{t} N(\mu, 1)}.$$

Normally distributed random numbers are generated with MATLAB's `randn` command.

The conductance equations $\frac{dg_S(t)}{dt} = (...)$ can be solved analytically in between incoming spikes $g(t) = exp(-t/\tau_s)/\tau_s$. Computing $g(t + \Delta t)/g(t)$ yields a recursive formula $g(t + \Delta t) = exp(-\Delta t/\tau_s) \cdot g(t)$ that can easily be implemented.

### 3.2.2 Single Neuron

As a first test for the implemented MATLAB routines (`CoupledIF`, see appendix) the reaction of a single neuron to a direct current without noise will be computed. It is

[36] Measures are obtained by comparing exact integration schemes that solve the equations at an arbitrary precision with standard Euler, improved Euler (interpolation of the spike timing to increase accuracy), second order Runge-Kutta (with and without interpolation of spike times) integration methods.

expected, that for an input above the threshold $I_{Th}$ the neuron starts to fire. The threshold current and the expected firing rate can be calculated analytically[37].

$$: I_{Th} = \frac{V_{Th} - E_L}{r_m} \tag{33}$$

$$r = \left[\tau_m ln\left(\frac{r_m I + E_L - V_{Res}}{r_m I + E_L - V_{th}}\right)\right]^{-1} \tag{34}$$

$$r \approx \frac{E_L - V_{Th} + r_m I}{\tau_m (V_{Th} - V_{Reset})}. \tag{35}$$

The equations for the firing rate are only valid if $I(t) > I_{\mathrm{Th}}$.
Used parameters of the simulation were:

| | |
|---|---|
| $V_{Th}$ | -54 mV |
| $V_{Res}$ | -80 mV |
| $\tau_m$ | 20 ms |
| $E_S$ | -80 mV |
| $r_m$ | 1 |
| $\Delta t$ | $10^{-3} ms$ |
| $I(t)$ | $0...100 mV$ |

The firing rate was determined by counting the number of spikes occuring in an interval of 1 second. Numerically calculated (blue) and analytically predicted (green) firing-rates are nearly identical. Small differences stem from the fact that the simulation ran only for 1 second. One can see, that the approximate relationship for the firing-rate has the correct slope but underestimates the actual firing rate. To approximate the actual input current-firing rate relationship one could extend the function $F(I) = [I - I_{Th}]$. But because of the unknown relationship between the time constants in the I&F and rate model the comparison will only be possible on a qualitative basis and therefore this extension, that does not add to the qualitative behavior is not necessary.

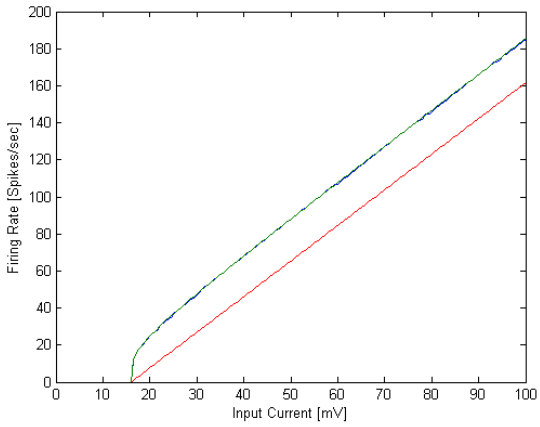


Figure 11: Input - firing rate relationship for a single neuron. Blue – numerical result. Green – exact formula. Red – approximate formula.

[37] [6] p. 164

If the interspike interval of the u-neuron crosses a threshold, that is determined by the synaptic time constant, the linear summation of spikes at the feedforward-synapse projecting onto the v-neuron comes into effect. The synaptic conductance can not return to zero in between spikes anymore. Instead after a transition it settles period to a time course with maximum conductance $> 1$ and minimum conductance $> 0$. This property of the synapse model is seen in figure 12.

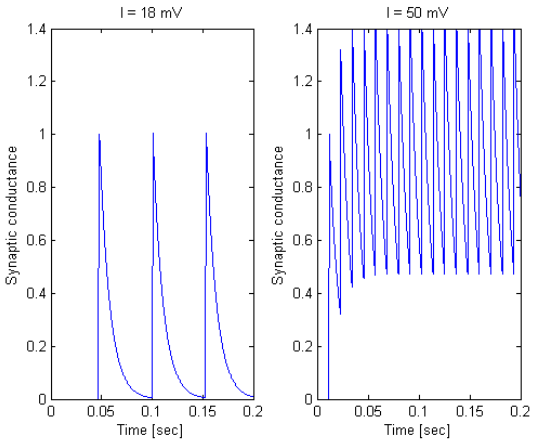


Figure 12: Comparison of synaptic conductance for different input strengts.

### 3.2.3 Coupled Neurons

The system of two coupled I&F neurons shows a distinct behavior, depending on the strength of feedback, the self-excitation and the choice of the membrane time constants. Now the influence of those parameters on the firing patterns will be investigated, using the results obtained in the rate model as a rough guideline.
First the stabilizing effect of feedback is shown. If there is no feedback, the firing-rate will increase rapidly at the beginning of the simulation due to the self-excitation of the u-neuron, see table 6, left plot. If feedback is introduced, the v-neuron "pulls down" the activity of the overactive u-neuron from time to time, causing its rate to fluctuate. The bursts that occur in LGN-neurons are similar to the behavior that can be observed for the u-neuron in the presence of negative feedback, see table 6, right plot. A number of spikes occur within a short period of time followed by silence. This behaviour is only possible, if the time-constant of the v-neuron is large enough: Because of the slower timescale and an appropriate strength of the feedforward connections it takes a number of spikes from the u-neuron before the v-neuron fires a single spike, that pulls down the membrane potential of the u-neuron and delays the firing of the next spike.
What happens, when in the presence of feedback the self-excitation is to high? Counting the number of spikes that occur in a time-window of one second as a function of the strength of the self-excitation gives a good impression. See the left figure in table 7. Clearly 2500 spikes/sec is beyond the behavior observed in real neurons. Therefore the self-excitation will be set to a strength of 6.
Now what influence has the feedback-strength on the number of spikes that are fired? The right figure in table 7 indicates, that the stronger the feedback, the smaller the number of spikes that arrive at the V1-neuron. This can easily be explained by the fact, that a

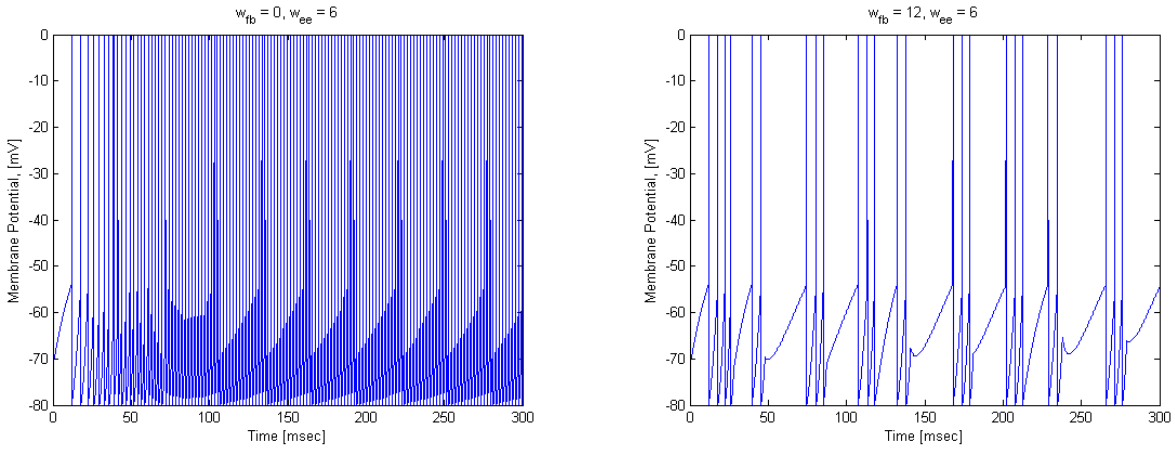


Table 6: Spiking behavior for u-cell of the two-cell model with self-excitation. Left – Without feedback. Right – With appropriate feedback.

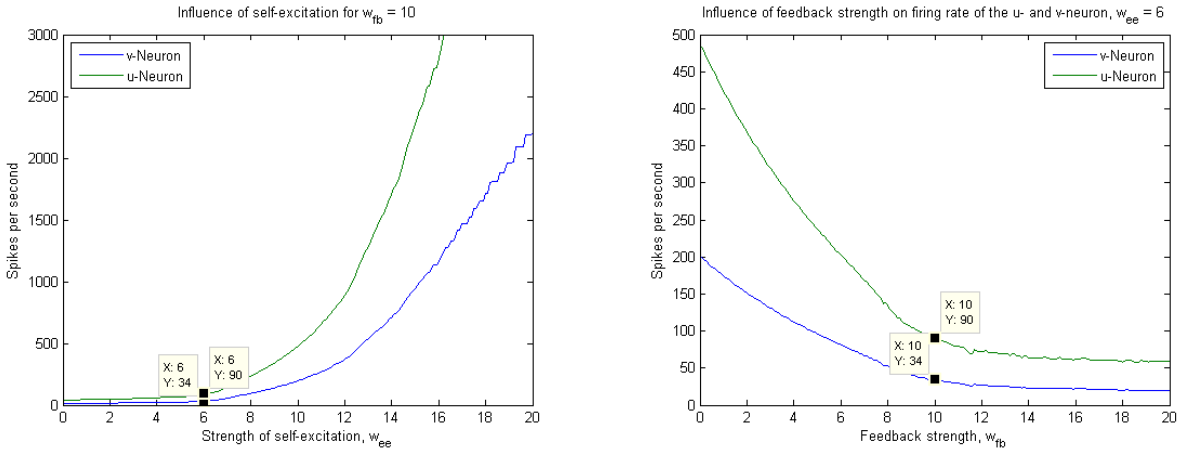


Table 7: Left –Influence of self-excitation. Right – influence of feedback strength on the firing rate of the v-neuron.

stronger feedback causes a deeper dip in the membrane potential of the u-neuron, that then takes longer to recover. Not surprisingly also the number of spikes fired by the u-neuron (green graph) goes down as the feedback is increased.
Another question that will be relevant for the phase of firing code is, how the oscillation frequency of the firing rate of the v-neuron depends on the strength of the input current injected into the u-neuron. In order to evaluate that, first the concept of an oscillation frequency for the firing rate has to be defined. The obvious case of an oscillation is a sinusodial time course, unfortunately the firing rate does not always behave in that way. In the current setup of the two cell model with a noisy input current there are two extreme cases. Suppose, there was no noise in the input current, then the neural response function of the v-neuron would be the same for every trial. According to the definition of the firing rate introduced in chapter 2.5.1, the identical spike-trains have to be added up and divided by the number of trials to obtain the firing rate. The probability distribution for the firing rate becomes a delta-distribution. Looking at the leftmost figure in table 8 reveals, that the Fourier decomposition of the firing rate is then also made up of delta impulses of equal height. Clearly no frequency dominates. The other extreme case is a completely noisy

input signal, also shown in the right figure in table 8 for which the Fourier decomposition also reveals no dominating component. Fortunately parameter combinations were found, for which oscillations can often be even made out from looking at the plots. The Fourier decomposition also shows a clear peak (table 9, left figure). Therefore it will be defined operationally for the application in this thesis:

> The frequency of the firing rate oscillation is the component of the Fourier decomposition of the firing rate signal that has the highest power.

A routine that runs a Fourier-decomposition for a given recording and determines the main frequency component has been developed[38] and is used throughout this thesis. This frequency can now be detected automatically.
From table 9, right figure, one can see that the oscillation frequency of the firing rate of the v-neuron is steadily increasing with increasing input current into the u-neuron. At a certain threshold a second frequency emerges, that then dominates the spectrum and is therefore detected as the main oscillation frequency.
Another phenomenon that can be observed in the two-cell-model is the emergence of an oscillation for an above-threshold input current $I(t)$. For $I(t) < I_{\mathrm{Th}_u}$ the system is only governed by the noise injected into the u-neuron and the v-enruon fires completely random Once the input is abov the threshold, a reliably dominating frequency can be detected in the spectrum. In the language of dynamical systems this is a bifurcation with bifurcation parameter $I(t)$ that causes the system to enter a limit cycle.
Finally the dependence of the oscillation frequency on the strength of the feedback connections is determined. The left figure in table 11 shows this relationship. As long as the feedback effects are weaker than the self-excitation of the u-neuron, the detected frequency is very high (170 Hz), since the firing rate of the u-neuron "blows up" and also drives the v-neuron into a state of high frequency. The strict application of the definition of the oscillation frequency of the rate-oscillation does not allow to detect this frequency until $w_{\mathrm{fb}}$ reaches 2. Looking at the spectrum of the firing rate for those feedback strengths (not shown) reveals, that though a peak exists for $w_{\mathrm{ft}} = 0$ and $w_{\mathrm{ft}} = 1$ around 180 Hz the mean (0 Hz) is stronger. For increasing feedback strength one sees a strong descend of the detected oscillation until $w_{\mathrm{fb}}$ has about the strength of the self-excitation. After that decrease, for values of $w_{\mathrm{fb}}$ above 11 the decay of the detected frequency is much narrower.

## 3.3 Comparison of the Rate Model and the Spiking Model

The two cell model spiking I&F neurons has been set up so that the firing rate it generates, oscillates. Comparing the numerical results with the predictions of the rate-model reveals the strengths as well as the shortcomings of the analytical approach.
The spiking model only generates a continuous rate-signal if noise is used, otherwise spikes will always occur at the same time and the rate signal obtained from averages over trials will only consist of isolated $\delta$-spikes. It was shown in table 8, left image, that such a signal will not exhibit clear peaks in the spectrum and an oscillation frequency according to the definition given can not be found. But though noise is needed, the effects of its strength can not be checked with the rate model, since it does not contain a noise term.

[38] See appendix for some details on the Fourier decomposition of signals with finite recording time and MATLAB function MainFreqComponent.

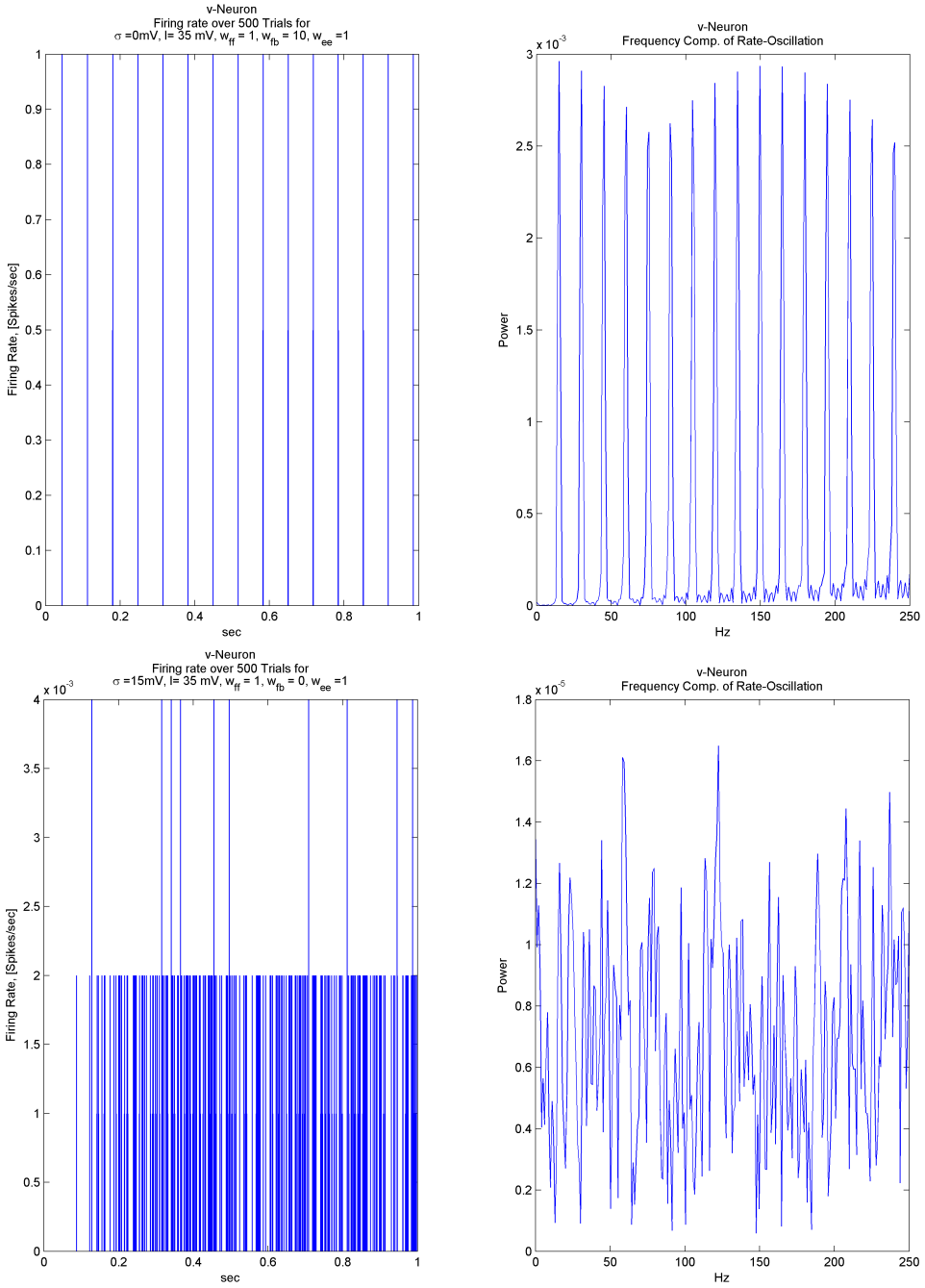


Table 8: Left – Fourier decomposition for the firing rate signal without noise, frequency components of uneven height are due to the finite recording time. Right – Fourier decomposition for a very noisy firing rate signal.

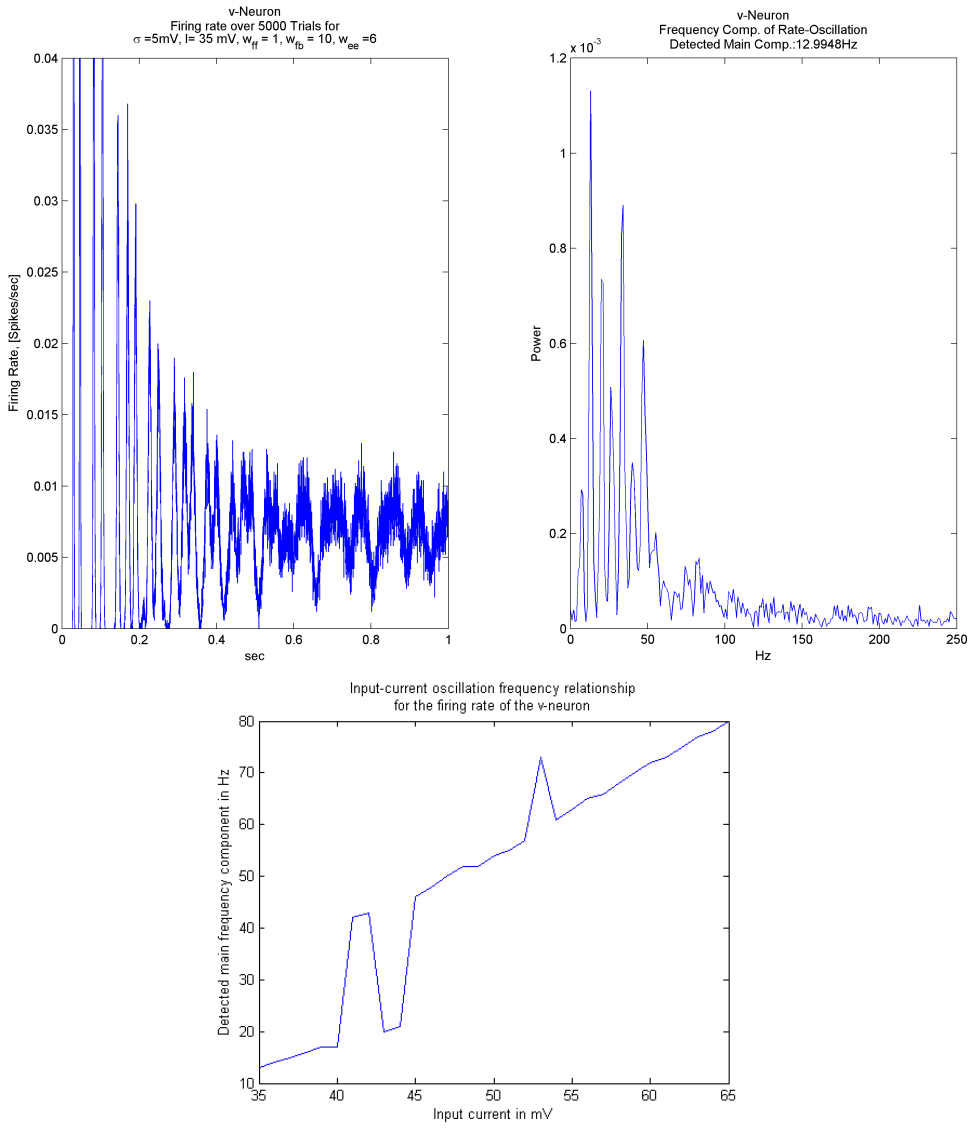


Table 9: Left – Nicely oscillating firing rate. Right – Detected oscillation frequency as a function of the input current.

| | u-Neuron | v-Neuron |
|---|---|---|
| $V_{Th}$ | -54 mV | -54 mV |
| $V_{Res}$ | -80 mV | -80 mV |
| $E_L$ | -70 mV | -70 mV |
| $\tau_m$ | 20 ms | 60 ms |
| $E_S$ | -80 mV | 0 mV |
| $V_{\mathrm{Sp}}$ | 0 mV | 0 mV |
| $r_m$ | 1 | 1 |
| $\tau_S$ | $\tau_{S_{\mathrm{fb}}} = 10ms$ | $\tau_{S_{\mathrm{ff}}}$=10ms |
| $\tau_{\mathrm{delay}}$ | 0 ms | |
| $w_{\mathrm{ff}}$ | 1 | |
| $\Delta t$ | $10^{-3}ms$ | |
| $I(t)$ | $35mV$ | |

Table 10: Parameters used for numerical simulations.

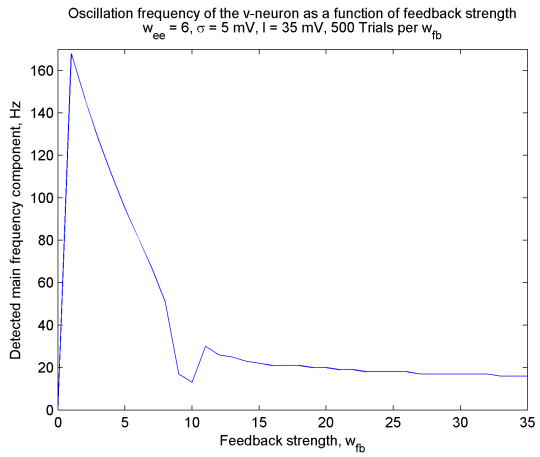


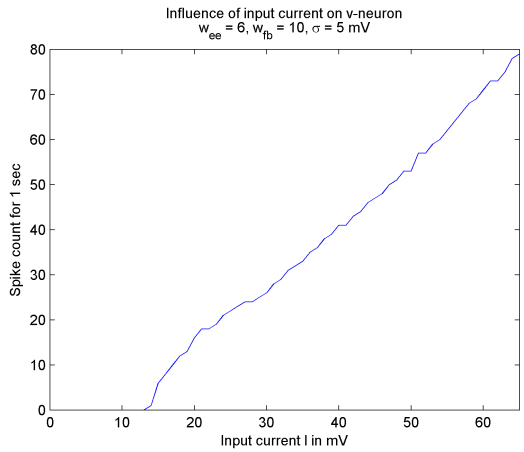


Table 11: Left – Influence of feedback strength on oscillation frequency of firing-rate of v-neuron. Right – Influence of input strength on number of spikes per second of v-neuron.

The emergence of oscillations occurs once the input to the u-neuron is above the threshold $I_{\mathrm{Th}_u}$ and nicely fits into the picture of the Hopf-bifurcation described in chapter 3.1.
The predicted danger of "explosions" of the firing rates in the absence of feedback were visible in the spiking model for example in the left figure of table 6, table 7 or the relationship of feedback-strength and oscillation frequency, left figure in table 11. Knowing this makes it easier to choose appropriate feedback strengths. Explosions as a result of too large $\tau_v$ could not be observed therefore no plots were included.
The analytical rate model correctly predicts the increase of the firing rate with increasing current. However it does not explain why the detected frequency of oscillation increases as the current is increased (table 9, right image). To incorporate this effect into the rate model, the imaginary part of the eigenvalues which determines the oscillation frequency would have to be dependent on $I(t)$. This is not possible with the current analytical model. The decrease of the firing-rate for the v-neuron as feedback is increased (table 7, right image) is correctly predicted by the analytical model, while the behavior of the oscillation frequency is contrary to the results obtained from the rate model. The oscillation frequency decreases in the spiking model but would increase in the rate model with increasing feedback strength (table 3, imaginary part of the eigenvalues for $w_{\mathrm{fb}} = 1$ and $w_{\mathrm{fb}} = 10$).
So the dependence of the frequency of the rate oscillation on feedback strength and the input current is clearly a problematic point. This might be explained by the fact unlike the firing rate itself the concept of a rate oscillation is not firmly defined and the rule introduced here, though reasonable, does not correspond to the oscillation caused by Hopf bifurcation described in chapter 3.1.
Fitting the rate-model to the presented results of the spiking model which were correctly predicted might allow to determine a heuristic relationship between the membrane time constants and the synaptic weights in both models.

## 3.4 Using the Spiking Model for Information Transmission

Having set up the two cell feedback loop in a way that creates oscillations, the two different coding schemes will now be tested. New rules for the assignment of neural

signals to symbols of the code will be motivated biologically and tested numerically for their ability to improve the transmission. Mechanisms that enable that improvement will be discussed in chapter 3.6. But first two measures have to be introduced that allow a quantitative comparison of both codes.

### 3.4.1 Measures for Comparing Codes

To compare the ability of the rate code and the phase of firing code to transmit information in the presence of noise, the mutual information as a basic measure is used:

$$I_M = \sum_s \sum_r P[r|s]P[s]log_2(\frac{P[r|s]}{P[r]}).$$

In the following simulations the stimuli "s" are two input currents of different strength $I_1$ and $I_2$ with difference $\Delta I = I_2 - I_1$. The stimuli will be shown with the same probability $P[s_1] = P[s_2] = 0.5$.
The symbols "r" of the code are the same for the rate code and the phase of firing code. They consist of a rate part and a phase part, that are combined and saved in an integer number. This number is determined in the following way:

1. A reaction of length $T = n \cdot 1/f$ beginning at $T_{Start}$ will be cut out from the neuronal response of the v-neuron. $f$ is the oscillation frequency of the reference signal. $n$ allows for more than one period of the reference signal. The maximum number of spikes that can possibly occur in this interval $a_{max}$ is technically limited by the time step width $\Delta t$ of the numerical method ($a_{max} = \frac{T}{\Delta t}$), but will generally be much lower due to biological limitations that are also incorporated into the model – the membrane time constants of the neurons and the synaptic time constants.

2. The number of spikes a, ($a \in 0...a_{max}$) in the window of length T is calculated.

3. For the rate code a random phase p, ($p \in 1...p_{max}$) is assigned to the reaction, for the phase of firing code the phase $p$ is determined by a rule. Two rules will be compared in the following chapter for the POF code. The number of phases $p_{max}$ is chosen to be four.

4. The symbol $r$ receives the integer value $r = a + (p-1) \cdot a_{max}$.

The probabilities $P[r|s]$, $P[r]$ are estimated from their relative frequenccy in histogram obtained from a number of trials using MATLAB's `hist` command with a number of bins that guarantees that every symbol has its own bin. In order to correctly estimate $I_M$ the probabilites of all possible reactions $r$ have to be determined. Reactions with a very high number as well as reactions with a very low number of spikes within the window occur very seldom. This makes it necessary to run a large number of trials. In theory an infinite number of trials would be necessary to estimate $I_M$ correctly. Due to limited computing resourcees usually 500 trials were obtained. For the entropy rate $\dot{H} = \frac{I_M}{T_s}$ of a single spike train of length $T_s$ Strong et al. [24] developed methods to interpolate the obtained mutual information (information rate) to the limit of infinite samples. This could also be done for the number of trials in the simulation. Without this interpolation the mutual information calculated here would be a lower bound for the actual mutual information between the input stimuli and the output symbols because very rare symbols might not be observed in

the limited number of trials. However, due to the limited number of trials that are used to sample $P[r]$ the mutual information calculated here can carry a bias called the "limited sampling bias"[39]. Therefore the actual mutual information might also be lower than the one calculated here. The effects of the limited sampling bias will not be quantified in this thesis.
What are important properties of a communication channel?
The speed of information transmission is measured by the *entropy rate* mentioned above. This quantity tells how long it takes to transmit a certain amount of information. The entropy rate will be of no concern here.
Background activity in the human brain is modeled as stochastic noise in the two cell model. How strongly does the increase of noise influence the capability of the neural coding channel? This relates to the *robustness* of a system. If a system also performs its task when parameters are varied, it is a *robust* system[40]. It would be a nice property of the two cell model, if using the phase code could for example make the neural communication channel "more robust". While the mutual information is a measure of how much the maximum possible information transmission is influenced by noise, in some cases perfect reliability is necessary. Shannons channel coding theorem[41] states, that this is generally possible up to a certain speed which is limited by a measure called the channel capacity, but does not tell how this can be implemented. To achieve perfect reliability sending the same message a number of times, using error correction at the receiving end of the channel, sending it once and waiting for an answer that the message was received error-free or other methods might be necessary. The problem of constructing such a method will be circumvented by asking a question that is easier to answer in this context: How close can two stimuli (injected currents) be, in order to still be distinguishable by the symbols of the neural code given a setup of the feedback loop. While in physical measurements the *resolution* characterizes a measure instrument and is the minimum difference for which two quantities can still be distinguished[42], here the *coarseness* will be used to characterize a communication channel that is using different codes.[43]

> The coarseness $I_C$ of a neural coding channel is the minimum distance $\Delta I$ between two stimuli $I_1$, $I_2$ for which the mutual information reaches its maximum.

And in the language of mathematics:

$$I_C = min_{I_2 \in [I_1, \infty)} \; [I_M(I_1, I_2) = max \; I_M(I_1, I_2)] \tag{36}$$

Since two stimuli with same probability are used, the maximum mutual information is 1. The coarseness $I_C$ will generally be given in mV and will be used to evaluate the effects of

[39] `http://www.scholarpedia.org/article/Sampling_bias#The_effect_of_limited_sampling_on_the_determination_of_statistical_and_causal_relationships`

[40] "A system, organism or design may be said to be "robust" if it is capable of coping well with variations (sometimes unpredictable variations) in its operating environment with minimal damage, alteration or loss of functionality." `http://en.wikipedia.org/wiki/Robustness`, July 21st 2010

[41] [4]

[42] "Resolution – the smallest amount of input signal change that the instrument can detect reliably", `http://zone.ni.com/devzone/cda/tut/p/id/$\sharp$4439toc1`, July 21st 2010

[43] This quantity is defined here only for the application in the context of this thesis. It is dependent on many parameters of the neural system as well as the decoding method for the neural response. Coarseness in neuroscience apparently also has other meanings, see [5].

parameter changes for the two cell model, the length of the encoding/decoding window, the definition of a reference signal, the strength of noise and the difference between the rate code and the phase of firing code. The influence of these changes in the setup will generally be be visualized using diagrams with the stimulus difference $\Delta I$ on the x-axis and the mutual information $I_M(\Delta I)$ for those two stimuli on the y-axis. $I_C$ is the point on the x-axis for which $I_M(\Delta I)$ reaches 1.
Since it will happen, that the communication channel will have the same coarseness $I_C$ for rate code and phase of firing code, but the POF code will give a better performance (higher mutual information) than the rate code for some stimulus differences $\Delta I$ below $I_C$, another measure is introduced:
When increasing the stimulus difference $\Delta I_i$ in n steps up to $I_C$, for each step $i$ the difference between the mutual information calculated using a rate $I_{M_R}(\Delta I_i)$ and a POF $I_{M_P}(\Delta I_i)$ code is determined and summed up for all n steps

$$I_D = \sum_{i=1}^{n} I_{M_P}(\Delta I_i) - I_{M_R}(\Delta I_i).$$

This quantity $I_D$ will be called the *accumulated difference*[44]. If the POF code is not more informative than the rate code, this measure will be 0. If it is more informative, the measure will be greater than 0. It is most useful if phase of firing code and rate code show the same coarseness. It follows from the definition of the accumulated difference that a higher mutual information for the POF code for a single $\Delta I_i$ is enough to reach an accumulated difference larger than zero, even though for all other combinations of $I_1$ and $I_2$ the codes might perform equally well. It should be mentioned, that this quantity is larger if $\Delta I$ is increased in smaller steps. The resolution at which $\Delta I$ is increased will therefore be the same in all comparisons.

### 3.4.2 Rate Code

It will be shown, that the strength of the feedback and the noise have a strong influence on the coarseness of the communication channel. The parameters used in the simulations are given in table A.2 in the appendix.
Intuitively it is expected, that increasing the background noise of the input will make it harder to distinguish different inputs. Therefore the coarseness of the communication channel using a rate code should be the higher, the higher the noise is.
The plots in table 14 on page 50 confirm that expectation. The coarseness $I_C$ for increasing noise strength $\sigma$ is obtained graphically from the plots and given in table 12. In the absence of noise only the length of the coding window influences the coarseness (see table 26). The longer the window the smaller the coarseness. Ideally an arbitrary small change in the input current $\Delta I$ could be detected using the rate code, if the window was infinitely long and there was no noise.
How does changing the feedback influence the coarseness of the communication channel using the rate code?
As predicted by the rate model of coupled neurons, increasing the feedback strength will reduce the number of fired spikes in the I&F model, a fact that was already observed

[44] Accumulated mutual information difference between phase of firing code and rate code over increasing stimulus difference would be very cumbersome.

| $\sigma$, ($w_{\text{fb}} = 10$) | $I_C$ |
|---|---|
| 2 mV | 17 mV |
| 5 mV | 17 mV |
| 10 mV | 26 mV |
| 15 mV | 30 mV |

Table 12: Influence of noise on the coarseness of the rate code.

| $w_{\text{fb}}$ ($\sigma = 5mV$) | $I_C$ |
|---|---|
| 8 | 13 mV |
| 10 | 17 mV |
| 12 | 30 mV |
| 14 | 43 mV |

Table 13: Influence of feedback strength on the coarseness of the rate code.

in 3.2.3. Choosing a smaller feedback will allow the self-coupled u-cell to fire at higher rates and cause the v-cell also to fire at higher rates which increases the number of spikes occuring within the 1 second of simulation. This results in the fact that for the same $\Delta I$ the mutual information $I_M$ for the stimuli is higher when the feedback is low.
The choice of the window length for the rate code was determined by the cycle duration of the reference signal that will also be used for the phase of firing code in the next chapter. The onset $T_{\text{Start}}$ has to be a multiple of the window length in order to start at a point where the sinusodial reference signal begins its first phase again. It was set to $6 \cdot 77ms = 462ms$.

### 3.4.3 Phase of Firing Code

There are a great number of possibilities for creating the external reference signal that the phase of firing code relies on. While certain bands of the LFP are widely used in experimental studies and can be created artificially in larger networks, in the two cell model declaring the combination of some signals a LFP signal is hard to justify. Nevertheless the small two cell model has its advantages – the comparatively small number of parameters allows to explore a larger part of the whole parameter space and might reveal the mechanisms that also determine the behavior of larger networks.
Possible reference signals should be either directly extractable from the dynamical variables of the model (firing rates, membrane potentials, synaptic currents) or, if they are externally imposed on the model, this should be justified by biological facts. Here two different reference signals will be investigated.
The first possibility is using the frequency of the rate-oscillation of the neuron itself as the frequency of a reference signal. This can be justified biologically, since the v-neuron lies in V1 and is surrounded by other V1 neurons that are likely to have similar receptive fields. Therefore, if stimulated by an external stimulus, given appropriate feedback strengths, not only the firing rate of the v-neuron will start to oscillate but the other neurons that surround it will also oscillate at the same or similar frequency. In chapter 3.2.3 this frequency was already discussed and its dependence on the input current determined.
In this setup one only sees the activity of surrounding neurons as a reference that does not influence the behavior of the v-neuron. In a more realistic setup those surrounding

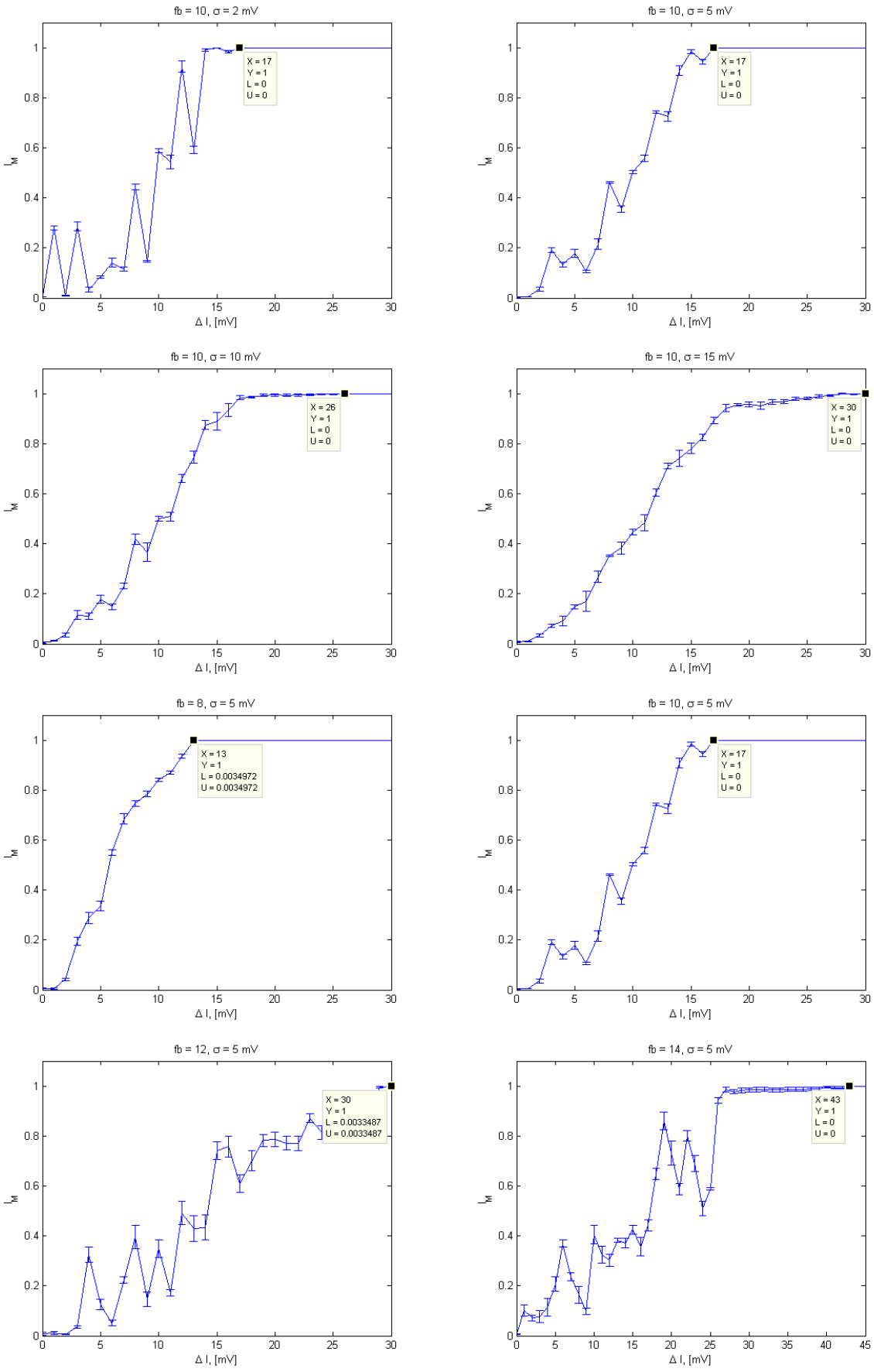


Table 14: Influence of noise and feedback on the $\Delta I$-$I_M$ relationship of the rate code.

neurons in V1 might also also give synaptic input to the v-neuron through recurrent connections. This input current again oscillates at a frequency identical or similar to the main frequency component of the rate oscillation. The oscillating input current in the model can be adjusted in terms of frequency, amplitude and noise. For the sake of simplicity this reference signal is directly injected into the cell but could also be modeled by spikes that are created by a Poisson process with varying rate arriving at a number of synapses of the v-neuron.
Those two different types of reference signals will be referred to as "non-influencing" and "influencing" or "injected" reference signal.
Other possibilities for reference signals not considered here could be:

- (Lowpassed) synaptic activity of the v-neuron.
- Weighted synaptic activity and membrane potential fluctuations of the v-neuron.

The question to be answered in both cases is, if the reference signal should follow changes in the oscillation frequency of the v-neuron that happen if the input current is changed or should keep its frequency. It is known from chapter 3.2.3, that increasing the input current will cause the oscillation frequency of the firing rate of the v-neuron to increase. Using the "surrounding neurons-argument" used before, the answer depends on the reaction of neurons surrounding the v-neuron in V1. Their oscillation can stem from two sources: either they have the same receptive field as the v-neurons, then if the stimulus changes, their oscillation period and therefore the frequency of the reference signal will probably change in the same way the v-neuron does. But if the surrounding neurons happen to have slightly different receptive fields and the input stimulus property only changes in that part of the receptive field of the v-neuron that is not part of the receptive fields of surrounding neurons, than the frequency of the reference signal will not change. Though this is rather a rather bold assumption, it will turn out to work best for the small model. Both cases will be checked and referred to as (non-)adapting reference signal or input (in)dependent reference signal.
For the case of an input independent reference signal the power spectrum of the firing rate obtained from 500 trials at $I = 35mV$, see table 9 left plot, gives the oscillation frequency for the reference signal. This frequency, $f = 12.99$ Hz will be the used for all other given input currents and determines the length of the encoding window, $T = \frac{n}{f} = n \cdot 77ms$. In their study in macaque monkeys, Montemurro et al. [12] used the delta band (1-4 Hz) of the LFP as a reference signal.
For the case of input dependent reference signals, the frequency of the reference signals will be obtained in the same way from 500 trials for each input current. It should be noted though, that not for all parameter combinations the rate oscillates so nicely as it does for the case given in the left figure in table9. Since the oscillation will occur at higher rates as the input current is increased, the length of the decoding window will shrink. The jumps in the detected oscillation frequency in table 9, right figure, will lead to a sudden decrease of the window size from one $\Delta I_i$ to the next $\Delta I_{i+1}$.
For all cases the reference signal is modeled as a sinusodial starting at the beginning of the decoding window that is extracted from the simulation with $T_{\text{start}} = 462ms$ (multiple of the oscillation period). In case of an adapting reference signal the onset of the window is chosen to start around 500 ms using `TStart = T*round(500/delta_t/T)`.

Suppose a window has been cut out from the recording and the position of the spikes is evaluated with respect to the reference signal. How is a phase-tag assigned to that part of the neuronal recording? At least to ways are possible:

- The phase with the largest number of spikes (`PhaseDistribution`-function, see appendix) determines the phase tag. If more than one phase reaches that maximum, the phase is chosen randomly among those.
- The phase in which the first spike occurs determines the phase tag. If no spike occurs, the phase is chosen randomly.

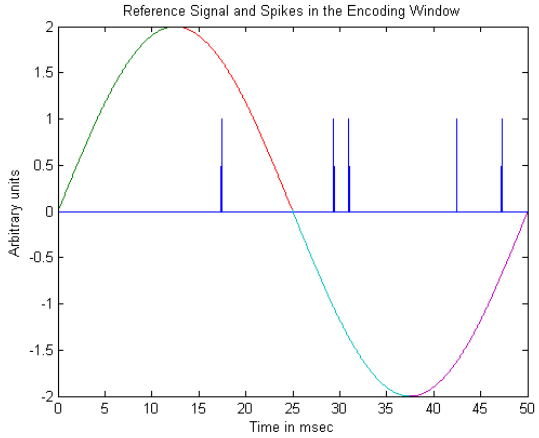


Figure 13: First spike-rule: the label given would be "Phase 2". Most spikes-rule: the label given would be "Phase 3" or "Phase 4" with equal probability.

A fourth option that will be available is the number $n$ of oscillation periods of the reference sign that make up the decoding window. We will see, that longer windows generally lead to a better performance. This option allows to check, whether the phase of firing code can also benefit from an extended window. The first spike rule will be applied to every single period in the window when more than one oscillation period is used. If the phase-tags differ for the periods, then the phase tag will be chosen randomly among the phases that were given.
The following numerical experiments will be run on the model in order to find the most suitable setup. The most suitable setup is one for which the phase code performs better (smaller coarseness $I_C$, or if the coarseness is the same, a higher accumulated difference $I_D$) than the rate code.

| | Option A | Option B |
|---|---|---|
| Reference Signal | Non-influencing | Influencing (injected) |
| Phase Tag | First spike | Most spikes |
| Frequency of Ref. Signal | Fixed | Adapting to input current |
| Nb. Osc. Periods | One | Multiple |

Table 15: Options that can be chosen for the encoding of phase code symbols.

There are several guidelines for running experiments in which one can change a number of factors[45] that influence the outcome of that experiment. In a *factorial experiment* all

[45] See for example [13]

possible combinations of the levels of the factors are investigated[46]. Two different options for each of the four settings lead to $2^4 = 16$ setups. But since properties like the amplitude of the reference signal that is injected into the v-cell, the amount of additional noise that is given, the feedback strengths, the amount of background noise and the number of oscillation periods, etc. can also be varied in small steps, the number of setups that have to be tested over 500 trials is even greater. This kind of experiment is beyond the scope of this thesis and also not necessary. For now it is sufficient to find one setup in which the phase of firing code consistently scores better than the rate code. It is possible that there exist other setups in which the POF code can perform even better than in the setups found here, but for a first exploration of the model this is not essential.
The comparisons between different setups for the POFC and the RC will be done in the order given in table 15, but contrary to a factorial experiment the choice (option A or B in the table) that has proven to bring better results, e.g. rule for phase tags will not be varied again in the next step, e.g. frequency of reference signal. The setup found in this way will then be checked for the influence of feedback and noise in the same way it was done for the rate code.
Since $I_C$ and $I_D$ vary even for 500 trials, their mean and standard deviation will be obtained from three runs. Standard deviations are indicated in the plots. $I_C$ is determined graphically from the $\Delta I$-$I_M$ plots using MATLAB's data cursor, the data tips for the points at which $I_M$ reached 1 is included in the plots. Since rate code and POF code will almost always be very close in their coarseness, the accumulated difference $I_D$ is more informative. $I_C$ for both codes can be determined at a higher resolution by increasing $\Delta I = I_{2_i} - I_1$ in smaller steps, but the plots indicate that this will not show a better coarseness for the phase of firing code since $\Delta I$-$I_M$ graphs for both codes become nearly identdical as they approach $I_M = 1$.
The coarseness and accumulated difference for the different options of the phase of firing code can be found in tables 19 to 22. For better illustration plots of one run for each comparisons is also included.

1. Non-influencing reference signal and influencing reference signal

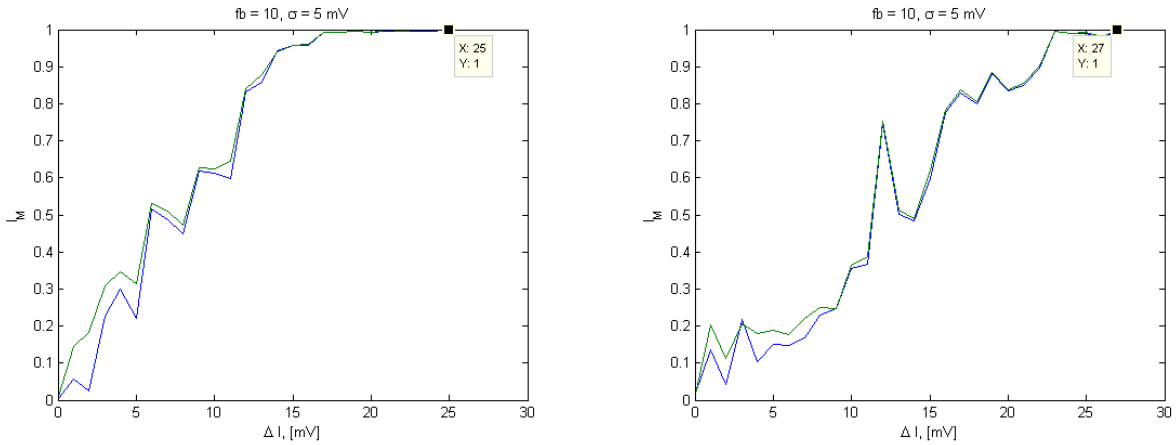


Table 16: Non-influencing reference signal and injected reference signal.

[46] [13], p. 506

With the parameters used, the non-influencing reference signal allows a smaller coarseness than the influencing and has at the same time a higher mean accumulted difference $\bar{I}_D$ (0.5727 compared to 0.3634). Therefore the non-influencing reference signal will be chosen. Whether the influencing reference signal might show a better performance for other amplitudes or phases of the injected current was not tested in more detail.

2. First spike rule and most spikes rule

   With the parameters used in this simulation the first spike rule performs better than the most spikes rule, see table left plot. The first spike rule has a mean accumulated difference of $\bar{I}_D = 0.7677$, while the most spikes rule showed only $\bar{I}_D = 0.5727$.

3. Fixed frequency and adapting frequency (changing window size, but shorter windows)

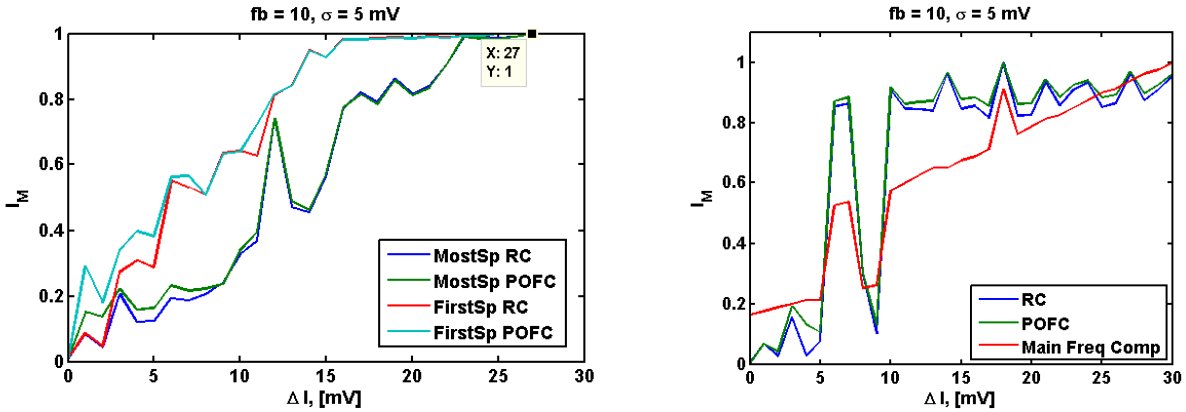


Table 17: Left – First spike rule and most spikes rule. Right – Adapting reference signal and detected oscillation frequency (in arbitrary units in that plot) that determines length and onset of the window.

The jump in the detected oscillation frequency has a strong influence on the $I_M$ calculations which can be seen in the right plot in table 17. This is explained by the fact, that the onset and also the length of the encoding window are now determined by the detected main frequency component (red line). Even though a higher frequency shortens the encoding window, the mutual information for most of the range of $\Delta I$ was higher for the adapting reference signal than for the fixed frequency signal. But even though for an adapting reference signal the mutual information grows faster, it does not reach 1 within the interval of $I_2$ tested here. If perfect discernability is not necessary, then the adapting reference signal should be preferred over the non-adapting. It also needs shorter time windows and can therefore (if the same results would also be true for other window onset times $T_{\text{Start}}$) achieve higher information rates (information transmitted per unit of time) at the cost of unreliable communication.

Since all setups here should make reliable communication possible in the sense that current differences above a certain limit should reliably cause different signals, the fixed frequency reference signal will be chosen.

4. Single period and multiple periods of the reference signal

Employing the first spike rule in this comparison of a single-period reference signal with reference signals of two and three oscillation periods one has to decide how to assign a phase tag if the first spikes occur in different phases of the oscillation periods. It is chosen, that the phase-label will be randomly assigned to one of the phases in which the first spike occured.

Even though the coarseness of the system decreases with increasing number of periods for the reference signal, the advantage of the phase code over the rate code is diminishing, for one period $I_C = 17mV$, $\bar{I}_D = 1.4326$, two periods $I_C = 12mV$, $\bar{I}_D = 0.3202$, three periods $I_C = 10mV$, $\bar{I}_D = 0.1755$. An increasing benefit of the phase of firing code for more periods can not be observed (see table 18 and 22). In the following therefore only one period of the reference signal will be used.

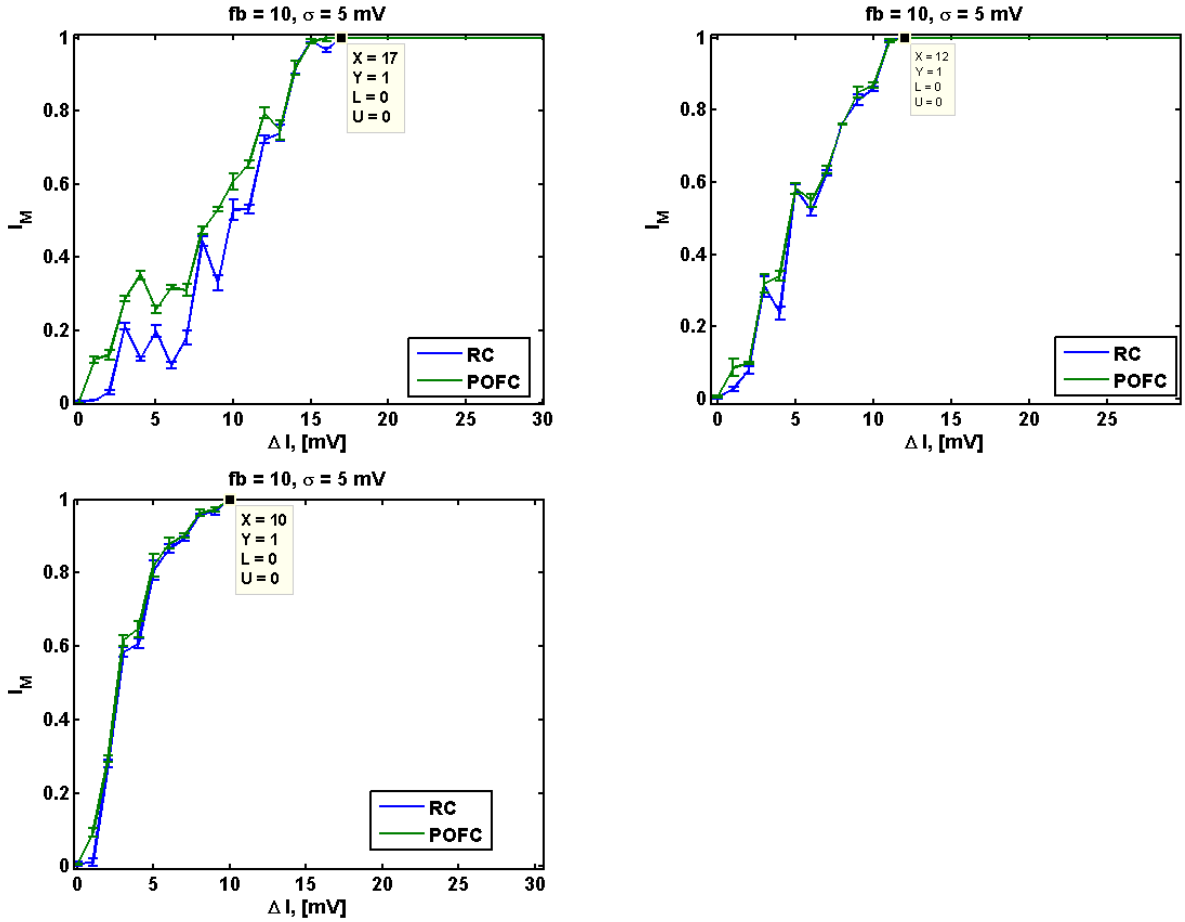


Table 18: Top left – Single period. Top right – Two periods. Bottom left – Three periods.

The following model will now be tested for the influence of feedback strength and noise:

- non-influencing reference signal
- first spike phase tag
- fixed frequency of reference signal
- one oscillation period.

| | Non-influencing | Influencing |
|---|---|---|
| Run 1 | $I_C = 25$ mV, $I_D = 0.6384$ | $I_C = 27$ mV, $I_D = 0.2502$ |
| Run 2 | $I_C = 17$ mV, $I_D = 0.4895$ | $I_C = 27$ mV, $I_D = 0.4553$ |
| Run 3 | $I_C = 17$ mV, $I_D = 0.5901$ | $I_C = 27$ mV, $I_D = 0.3748$ |
| Mean | $\bar{I}_D = 0.5727$ | $\bar{I}_D = 0.3634$ |

Table 19: Coarseness and accumulated difference for non-influencing vs influencing reference signal.

| | Most Spikes Rule | First Spike Rule |
|---|---|---|
| Run 1 | $I_C = 25$ mV, $I_D = 0.6384$ | $I_C = 25$ mV, $I_D = 0.7040$ |
| Run 2 | $I_C = 17$ mV, $I_D = 0.4895$ | $I_C = 17$ mV, $I_D = 0.8012$ |
| Run 3 | $I_C = 17$ mV, $I_D = 0.5901$ | $I_C = 25$ mV, $I_D = 0.7978$ |
| Mean | $\bar{I}_D = 0.5727$ | $\bar{I}_D = 0.7677$ |

Table 20: Coarseness and accumulated difference for first spike tag vs most spikes tag.

| | Adapting Reference Signal | Fixed Reference Signal |
|---|---|---|
| Run 1 | $I_C =$ not determinable, $I_D = 0.6849$ | $I_C = 25$ mV, $I_D = 0.7040$ |
| Run 2 | $I_C =$ not determinable, $I_D = 0.7345$ | $I_C = 17$ mV, $I_D = 0.8012$ |
| Run 3 | $I_C =$ not determinable, $I_D = 0.7583$ | $I_C = 25$ mV, $I_D = 0.7978$ |
| Mean | $\bar{I}_D = 0.7259$ | $\bar{I}_D = 0.7677$ |

Table 21: Coarseness and accumulated difference for fixed reference signal vs adapting reference signal.

| | One Period | Two Periods | Three Periods |
|---|---|---|---|
| Run 1 | $I_C = 17$ $I_D = 1.4253$ | $I_C = 11$ mV, $I_D = 0.2771$ | $I_C = 10$ mV, $I_D = 0.1571$ |
| Run 2 | $I_C = 17$ $I_D = 1.3899$ | $I_C = 11$ mV, $I_D = 0.4184$ | $I_C = 10$ mV, $I_D = 0.1553$ |
| Run 3 | $I_C = 16$ $I_D = 1.4557$ | $I_C = 11$ mV, $I_D = 0.2651$ | $I_C = 10$ mV, $I_D = 0.2142$ |
| Mean | $\bar{I}_D = 1.4326$ | $\bar{I}_D = 0.3202$ | $\bar{I}_D = 0.1755$ |

Table 22: Coarseness and accumulated difference for one, two and three periods of the reference signal.

The experimental setup will be the same as in the test of the rate code. Noise or feedback will be varied, while the other factor is kept constant. The results are summarized in table 23 for the varying noise level and table 24 for varying feedback strengths. As for the rate code the coarseness decreases with increasing feedback strengths and noise level. A closer examination of the results follows in the next chapter.

| $\sigma$, $w_{\text{fb}} = 10$ | $I_C$ | $I_D$ 1st | $I_D$ 2nd | $I_D$ 3rd | $I_D$ mean |
|---|---|---|---|---|---|
| 2 mV | 17 mV | 1.25912 | 1.1815 | 1.21975 | 1.22013 |
| 5 mV | 17 mV | 1.31091 | 1.25195 | 1.28961 | 1.28416 |
| 10 mV | 28 mV | 0.841256 | 0.729015 | 0.433677 | 0.667983 |
| 15 mV | 30 mV | 0.234971 | 0.210509 | 0.227578 | 0.224353 |

Table 23: Influence of noise on the coarseness and accumulated difference of the phase of firing code.

| $w_{\text{fb}}$ ($\sigma = 5mV$) | $I_C$ | $I_D$ 1st | $I_D$ 2nd | $I_D$ 3rd | $I_D$ mean |
|---|---|---|---|---|---|
| 8 | 13 mV | -0.00762244 | -0.025152 | -0.0428368 | -0.0252037 |
| 10 | 17 mV | 1.31091 | 1.25195 | 1.28961 | 1.28416 |
| 12 | 30 mV | 2.26649 | 2.28238 | 2.52934 | 2.3594 |
| 14 | 44 mV | 1.09762 | 1.07595 | 1.13185 | 1.10181 |

Table 24: Influence of feedback strength on the coarseness and accumulated difference of the phase of firing code.

Finally the effect of the position and the length of the decoding window shall be illustrated. Two input currents of strength 35 mV and 45 mV will be given. First the decoding window will have a constant length of $T = 77ms$ and the calculated mutual information for a varying onset $T_{\text{Start}}$ of the window will be determined. The window will be situated at multiples of T from 462 ms to 847 ms. Then, to determine the influence of the window length the onset $T_{\text{Start}}$ will be kept constant at 462 ms as the T is increased from 40 ms to 190 ms. The results in table 26 show, that the POF code always performs better than the rate code regardless of the chosen window position, which affects the $I_M$ calculations only slightly ($I_M$ between about 0.45 and 0.65). The right figure in table 26 shows, that the longer the encoding window, the higher the mutual information. Therefore both codes improve with increasing encoding/decoding window length but the POFC has always a higher $I_M$ than the RC for a given window length.

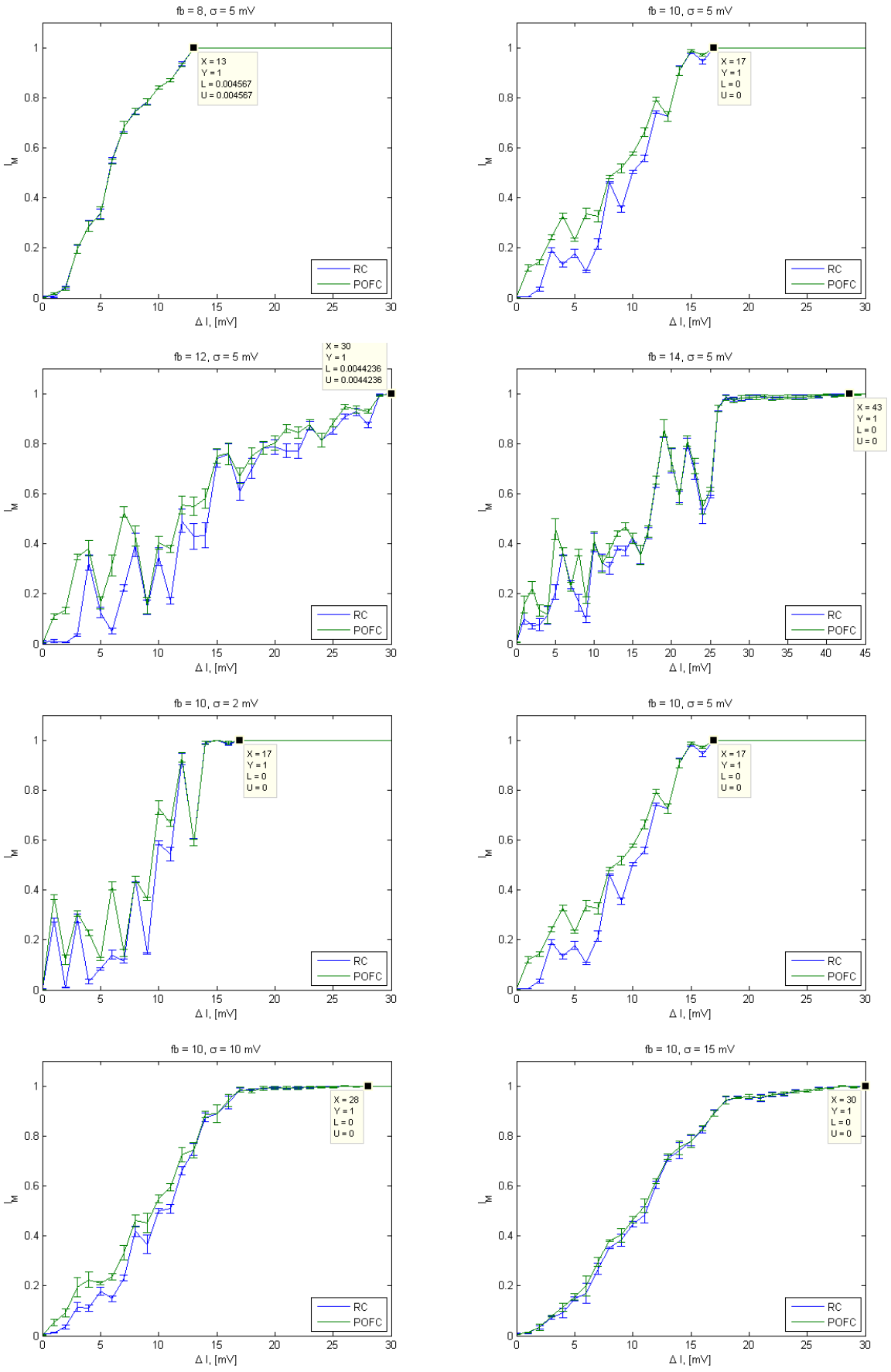


Table 25: Influence of feedback strength and noise strength on the $\Delta I$-$I_M$ relationship of the phase code.

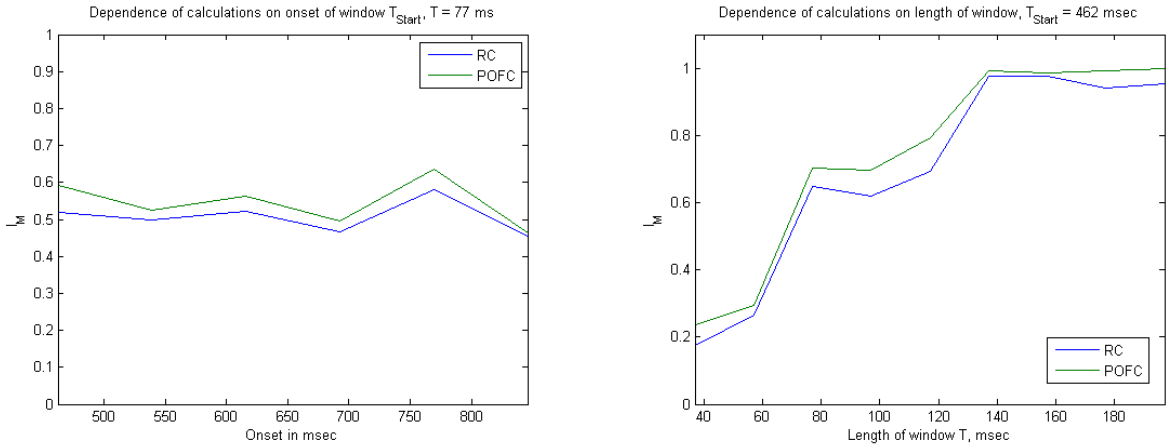


Table 26: Influence of onset and length of decoding window.

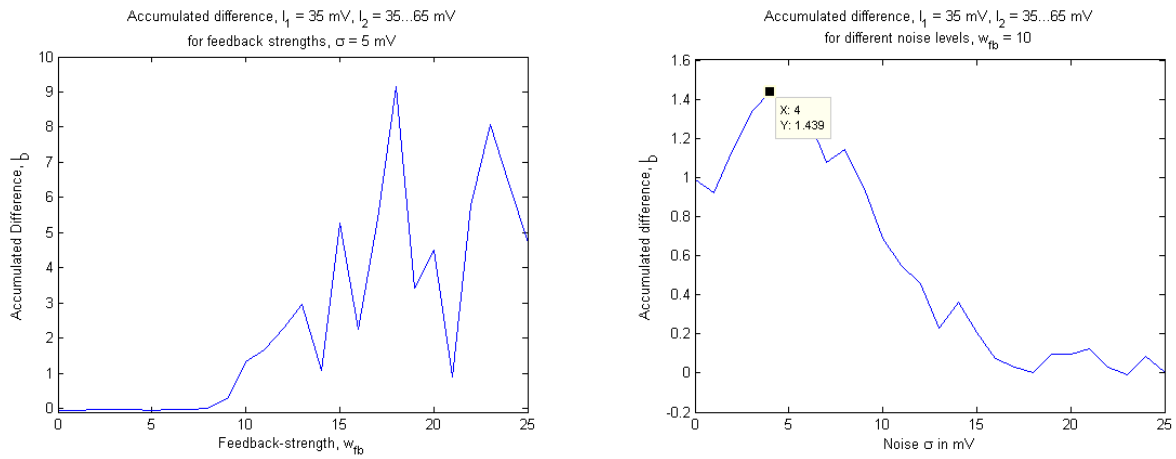


Table 27: Influence of feedback strength and noise level on the accumulated difference for the POF code.

## 3.5 Comparison of the Codes

The main factors that determine the performance of the neural feedback loop, noise and feedback strength have now been quantified for the rate code and the phase of firing code using the coarseness $I_C$ and the accumulated difference $I_D$ as a measure. Even though some effort has been made to determine a favorable setup for the phase code (source of reference signal, assignment of phase tag, frequency of reference signal, number of oscillation periods), for every combination tested here the phase code was never able to achieve a smaller coarseness than the rate code. Increasing the feedback strength always resulted in a higher coarseness of both codes, since fewer spikes were fired overall. An increase from $w_{\text{fb}} = 8$ to $w_{\text{fb}} = 14$ more than tripled the coarseness ($I_C = 13mV$ to $I_C = 44mV$). Increasing the background noise $\sigma$ had the same effect: the coarseness of the channel went up and was the same for both codes. In the experiments here the current $I_2$ was increased in 1 mV steps. This limited the accuracy up to which the coarseness of both codes could be determined. Hence it is possible, that the phase of firing code has a small advantage over the rate code, but the plots in table 25 (for example $fb = 14, \sigma = 5$) show that as the mutual information approaches 1, the difference between the rate code and phase of firing code shrinks. Therefore, if perfect discernability of stimuli is necessary, it does not matter which code is used.
However, if perfect discernability is not essential, the mutual information for the two stimuli does not have to reach 1, the phase of firing code can be much more informative than the rate code. Consider for example the case in table 25 with $fb = 12, \sigma = 5$. If the stimulus difference is around 11 mV, the rate code can achieve a mutual information of about 0.2 while the phase of firing code achieves twice as much, 0.4. Another example is the case $fb = 10, \sigma = 2$ with $\Delta I = 6mV$: $I_{M_{RC}} \approx 0.1$, $I_{M_{POFC}} \approx 0.4$. Unfortunately the advantage of the phase code is not consistent over the whole range of $\Delta I$s. For some choices of $\Delta I$ its advantage is close to zero ($fb = 10, \sigma = 2$ with $\Delta I = 8mV$). Looking at the accumulated difference $I_D$ between phase code and rate code obtained in the experiments as well as the left plot in table 27 gives a more general view of the advantages of the POF code. Leaving the noise constant, the POF code can take advantage of increasing feedback strength. Though (as mentioned) the overall coarseness of the communication channel decreases, $I_D$ increases. While for $w_{\text{fb}} = 8$ RC and POFC have nearly no difference at all ($I_D$ = -0.02), choosing $w_{\text{fb}} = 12$ leads to a striking advantage of the phase code ($I_D$ = 2.36) that is mainly due to the advantage for small $\Delta I$. Increasing the feedback further to $w_{\text{fb}} = 14$ leads to a lower $I_D$ = 1.10, that still shows the advantage of the phase code.
For increasing noise table 23 suggests, that the advantage of the phase code over the rate code decreases. Injecting only a small amount of noise ($\sigma = 2mV$) amounting to less then 10% of the injected current, makes a clear advantage of the POF code possible ($I_D$ = 1.22). Further increases in the noise up to about 50% of the injected current ($\sigma = 15mV$) lead to a decrease of the accumulated difference ($I_D$ = 0.22). The right plot in table 27 which shows the accumulated difference over a larger range of the noise strength $\sigma$ confirms that the advantage of the POF code is strongest for low noise around $\sigma = 4$ mV and decreases with higher background noise.
It has to be emphasized, that not the whole parameter space of the model was tested. The advantage of the phase code might be bigger or smaller with other choices of the neural time constants, the position of the decoding window, the strength of self excitation, et cetera. Chapter 3.7 will therefore give a conceptual overview of the model and its

parameters that can be helpful for more exhausitve exploration of the parameters and further analysis.

## 3.6 Suggested Mechanisms

Up to now the investigation of the two codes was purely descriptive. In this section some mechanisms that made the higher mutual information for certain stimlus differences $\Delta I$ for the phase code and therefore $I_D>0$ possible will be discussed, this includes the effects of the window position and of the window length.
To distinguish two stimuli, the symbol r that is constructed from the number of spikes in the time window $[T_{\text{Start}}, T_{\text{Start}} + T]$ and the phase tag as described in chapter 3.4.1 has to be reliably different for the two stimuli. First a case without noise will be described:
Assume that the frequency of the reference signal was constant, not influencing the neural feedback loop, the first spike rule was applied and the window had a constant onset and length. From the analytical description of the rate model as well as the simulations in chapter 3.2.3 it is known, that the number of spikes fired within one second of simulation will increase with increasing input current. Therefore the existing spikes have to move "closer together". Figure 15 illustrates this effect idealistically[47]. An increase from I = 35 mV (A) to 45 mV (B) leads to a shift of the first spike within the window from phase 4 to phase 3. The spike that lay to the right of the window moved closer but still does not occur within the window. The spike-count stays constant while the phase-label changes. Therefore this change in the input current can only be detected by the phase of firing code. The number of phases into which one period cycle is split (here: 4) determines how small an increase of I can be detected. Further increasing the input current (C) then finally causes the last spike to occur within the window. Now the rate-code can also signal the change in intensity.
Even though this kind of argumentation seems plausible there are a number of hidden assumptions about the dependence of spike-times on the input current that ought to be tested. At least for the increase from a sub-threshold input for which the system is noise-driven to an above-threshold input a simple shift of the spike times is not justifiable since the spiking patterns change totally. If the current lies above this threshold and the system oscillates, one still has to assume that the intervals in between two spikes change uniformly for increasing input currents to use the proposed mechanism as an explaination.
The mechanism shown in figure 15 would lead to a smaller coarseness for the phase of firing code. This was not observed, so why was the POF code in none of the cases able to achieve a lower coarseness than the rate code? One reason might be the high firing rate: If the firing rate is high, there will almost always be a spike in the first phase of the reference signal. The mechanism suggested in figure 15 only works, if no spikes occur in the first phase so that the spikes occuring in later phases can move forward as $I$ is increased. The "most spikes rule" was supposed to alleviate this shortcoming, hoping that there was another yet unforseen mechanism, but also failed to bring about the desired result.
The effect of increasing feedback-strength on the coarseness can be depicted using the same concept of the "missing spike". It was shown analytically and numerically that increasing the feedback reduces the firing rate of the v-neuron. Therefore, generally speaking the time in between spikes will be longer. This means, that the missing spike lies further away from the end of the window and it will take a greater increase in the input current to let it occur within the window. This nicely explains why the coarseness increases as the feedback is increased.

[47] The input currents are only for illustration and have not been checked in experiment.

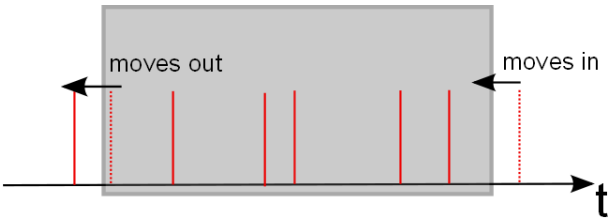


Figure 14: Explaining the jagged shape of the $\Delta I$-$I_M$ relationship.

In the two cases described so far the mutual information for the two stimuli $I_1$ and $I_2$ would jump from 0 to one once the stimulus reached the threshold and the missing spike entered the window. But the $\Delta I$-$I_M$ plots showed a rather slow increase in mutual information from 0 to 1 for changes in $\Delta I$ of about 10-35 mV. Now noise has to be taken into account. As the left figure in table 9 which is the sum of neural spike trains over 5000 trials shows, at the beginning of the recording the variance in spike timing is small, therefore spikes occur at nearly the same time in many trials. The deviation from the spike-timings that would be obtained without noise grows as the simulation proceeds. With noise the "missing spike" occurs in the window for some trials and outside for others. This prevents $I_M$ from jumping directly to 1. The stronger the noise the larger the variance of the spike-time for the missing spike. Even if the mean of the spike time lies already far within the window, the large variance still causes some of the spikes to fall outside of the window in some trials thereby necessitating a larger input to reach $I_M = 1$. This explains, why higher noise increases the coarseness.
Possibly because the spike variance increases over time, the mutual information increases if the window is placed further to the right. Compare left figure in table 26. For the window at the beginning (462 ms) $I_M$ is larger than at the end (847 ms). The sudden jump in $I_M$ for $T_{\text{Start}} = 770$ ms can not be explained, though.
Why does the window length affect the $I_M$ calculations (see right figure in table 26)?. One can see, that the longer the time window, the higher the mutual information of the coding channel. In table 11 in chapter 3.2.3 one saw, that for a window of one second, the relationship between the spike count for the v-neuron and the input current is linear and it is obvious, that for an even longer window, the the relationship will be the same. This long window averages out fluctuations of the firing rate that occur at around 10-30 Hz. For the shorter windows (40 ms to 200 ms used in the table 26) increasing the lenght improves the estimation of the average rate. Since this average rate has has a linear relationsip with the input current a better estimate of the average rate leads to a better estimate of the current, which enables a higher mutual information.
Another open question is the reason for the jagged shape of the $\Delta I$-$I_M$ relationship. This is most likely caused by choosing the window to start at a fixed point in time $T_{\text{Start}}$. For increasing currents the number of spikes within the window is increased if spikes that formerly lay to the right of the window fall now within the window ("missing spike"). At the same time the decreasing interspike interval causes spikes that lie close to the left limit of the window to leave the window. Therefore increasing the input current can also lead to a decrease of the spike count within a small range of $\Delta I$. This occurs, if the left spike leaves the window before the right one enters it.
All of these arguments can be made more rigorous using interspike interval distributions

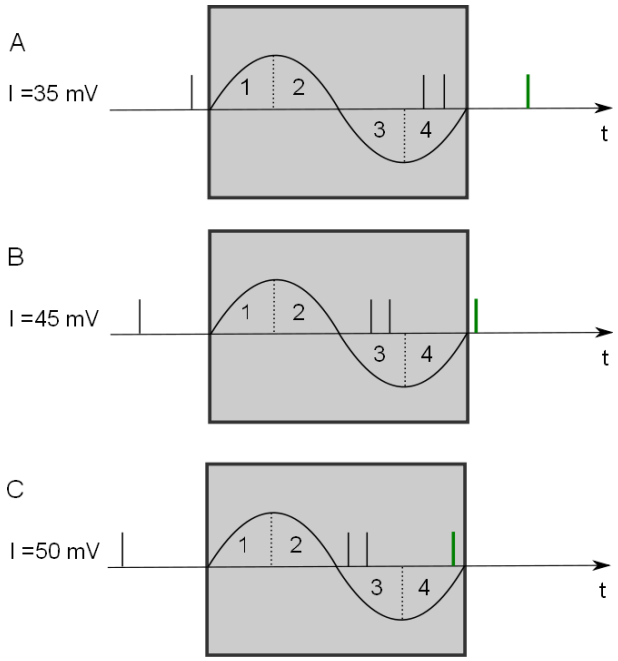


Figure 15: Mechanism behind the phase code. Green – "Missing spike".

and statistics for the phase-distribution of spikes within the window[48] that might be either analytically obtainable from the model of I&F neurons with noise or sampled from trials.

[48]See MATLAB function PhaseDistribution in the appendix

## 3.7 A Different View on the Two Cell Model

During the course of this thesis it became apparent, that in order to describe the way in which information is passed along the feedback-loop, especially the influence of the many parameters that can change the performance of the system, concepts from communication systems can be very useful. Having already explored some of the properties of the two cell model, this section uses concepts from communication systems to put the way in which the two cell model can be further explored on a more solid basis.
Shannon's theory of communication was already mentioned in chapter 2.5. Rieke at al. [19] developed methods to reconstruct a stimulus when the neuronal response of a cell is given. The setup in this thesis is somewhat more simplified. Instead of a real world stimulus that is being encoded in a spike-train by the retinal ganglion cells and then passed on to the LGN (1), a current is directly injected into the LGN cell. The task the V1 cells face is nevertheless the same – detect the stimulus (current injected) given the neural response. Two signals can be extracted from the v-neuron: its membrane potential $V(t)$ that also contains the spikes and the time course of the synaptic conductivity $g_V(t)$. These two signals contain the information about the stimulus. The decoding window, which was also mentioned in chapter 2.5 and the use of a particular neural code (RC, POFC) are enforced by creating a symbol (3) according some rule. Several of these rules have been explored already. This system works independently of the neural loop.
If the communication channel was free of noise, and the system (2) time-independent, the same current $I(t)$ would always lead to the same output signal. Due to the noise, different input currents sometimes lead to the same output signal and the same current sometimes to different output signals. This is why $\Delta I$ has to reach the threshold $I_C$ to prevent this mix-up from happening. The job of the decoder (4) is to minimize the uncertainty about the current that was injected. In chapter 3.4.1 the coarseness $I_C$ was proposed as a measure for the performance of the decoder. Finding a suitable reference signal, a rule for the assignment of phase labels, etc. all amounts to setting the properties of the decoder to values that minimize the coarseness.
The neural system itself has also a large number of properties that can be adjusted changing its response to inputs. Among the different responses are "explosions" of the firing rate if the synaptic strengths are not properly adjusted and oscillations of the firing rate, if the synaptic strengths and membrane time constants are chosen accordingly.
The reference signal (5) with the properties amplitude, frequency and phase can be constructed using different combinations of the output of the neural loop. To obtain the firing rate it is necessary to run the spiking model a number of times, to obtain the frequency of the oscillation, the Fourier decomposition is used. The created reference signal can be choosen to influence the neural system itself (influencing and non-influencing reference signal).
In the previous chapter 3.4.3 it became apparent, that the choice of the parameters for the symbol creation is crucial to the performance of the decoder. The goal is to obtain the set of parameters for which the decoder shows the highest performance (smallest $I_C$) and can, if neccessary, reconstruct the stimulus $I(t)$ as $I_R(t)$ while at the same time not exceeding biological limits (strength of reference signal, length of decoding window, ...) that would render the model inapplicable to the explaination of real biological phenomena.

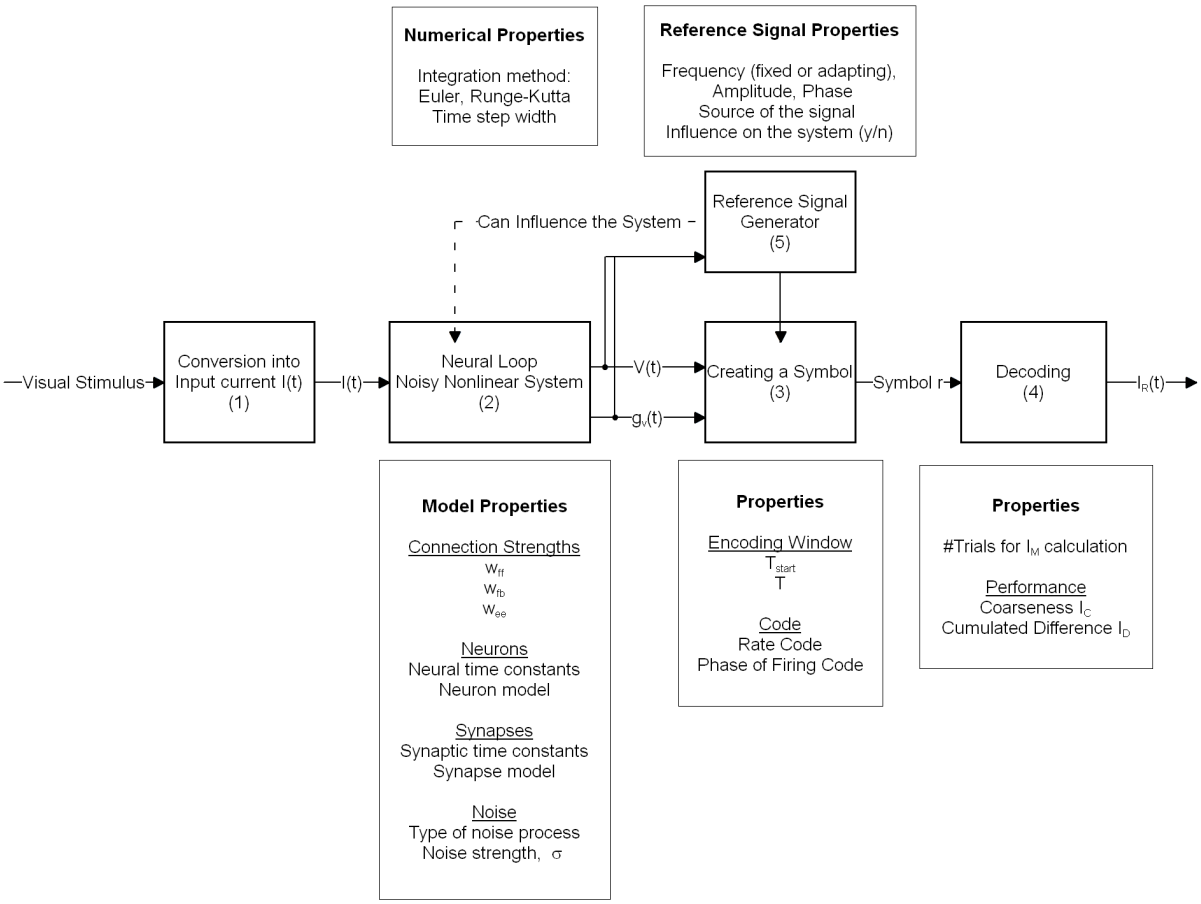


Figure 16: Seeing the neural feedback-loop as part of a communication channel.

# 4 Multi Cell Model

The initial motivation for looking at the two cell model was its relevance in the structured feedback connections between LGN and V1. This chapter presents a possible setup for a computer-experiment that might give insight into the application of a POF code in the presence of structured feedback. Of course it will exploit the fact, that the POF code for higher feedback strengths can reduce ambiguity when compared to the rate code.

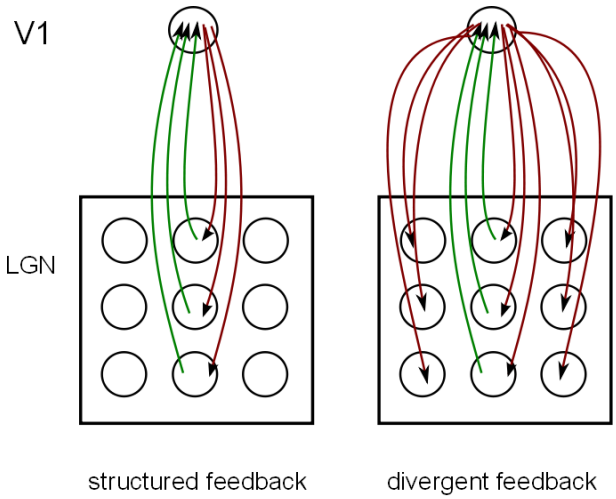


Figure 17: Possible cortical setup for the multi cell model. Green – excitatory feedforward; Red – inhibitory feedback.

The receptive field of the simple cell in V1 is determined by the structure of the feedforward connections. Therefore it will receive the strongest input, if a vertical bar (stimulus B) is presented. The left and the right case in figure 17 differ in the way feedback is given. The *structured* feedback on the left side could be implemented as strong ($w_{\mathrm{fb}} = 12$) inhibitory connections. The *divergent* feedback on the right side could be chosen weaker ($w_{\mathrm{fb}} = 8$). Yet another option is divergent feedback that has stronger feedback connections for the LGN cells that project onto the V1 neuron. In the classical Hubel-Wiesel model without feedback the firing rate of the V1-cell would be minimal for stimulus A and increase as the angle of the bar is changed toward the orientation of stimulus B. With feedback (structured as well as divergent) the V1 cell would fire at a higher rate for stimulus B as well. If for the horizontal bar only one LGN cell is activated and the feedforward strengths are chosen accordingly, the activity of the V1 cell can be driven mostly by the noise of the two non-stimuliated neurons similar to the case tested in the two cell model. This causes an irregular firing pattern for the V1 cell. If the other two LGN-cells receive input as well (vertical bar) they will fire more regularly which in turn will cause more regular feedback spikes and therefore oscillation of the V1 neuron. Frequency and amplitude (maximum and minimum firing rate) of that oscillation will be dependent on the strength of the feedback connections and therefore differ for structured and divergent feedback. The left figure in table 27 in chapter 3.4.3 showed, that the advantage (accumulated difference) of the phase of firing code over a rate code can increase with increased feedback strengths. For the two cell model this was especially prevailing for the change from $w_{\mathrm{wb}} = 8$ to $w_{\mathrm{wb}} = 12$. Therefore the phase code could be more useful in structured feedback connections than in unstructured, weaker feedback connections.

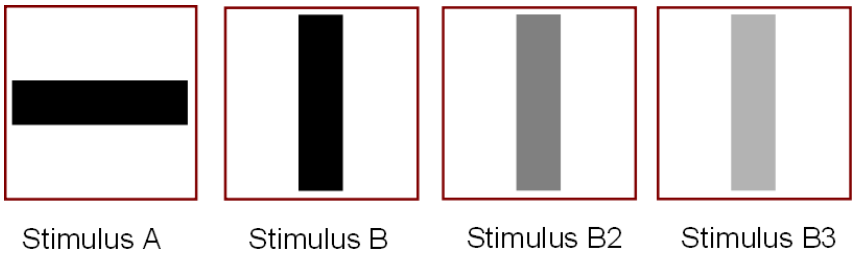


Figure 18: Different stimuli for the multi cell model.

The task of discriminating between two input currents $I_1$ and $I_2$ that was characterized by the coarseness and accumulated difference in the two cell model can now for example be changed into discriminating two bars of the same orientation and shape but different brightness (see figure 18). The brightness of the bar is changed in small steps starting from a reference-brightness B. Reference bar and altered bar (B2, B3, ...) are presented in random order and it is checked whether in this setup a POF code can show a higher accumulated difference, which means that it enables detection of smaller changes in the brightness for some brightness levels, or even a higher coarseness. The choice of a reference signal in this case can still be guided by the reasoning in chapter 3.4.3.
The results of the two cell model only suggest oscillating behavior and a possible application of the phase of firing code in this more realistic model. In the larger model one V1 cell receives input from a number of LGN-cells, therefore the input spike train might have a different temporal structure, since it stems from three neurons that, even though their activity is not completely uncorrelated due to the feedback, are less constrained in their firing patterns than single neuron. The time-difference between two incoming spikes is for example not governed by the reset of the membrane potential of a single neuron. Two spikes could even arrive at exactly the same time at the cortical neuron. This might cause different oscillation patterns for the cortical neuron and therefore different detected oscillation rates. The typical bursts that were observed in chapter 3.2.3 (table 6) might show a different shape which will affect the frequency components of the rate oscillation. Generally speaking with a larger number of neurons one will be able to create a much richer dynamic behavior. To make definitive statements about the advantages of a POF code in the multi cell model implementation is indispensable.

# 5 Discussion

"Ever tried.
Ever failed.
No matter.
Try again.
Fail again.
Fail better."

— Samuel Beckett, Worstward Ho.

The claim put forward in the introduction could not be supported fully in this thesis. The coarseness of the neural communication channel using a phase code does not differ substantially from a rate code. Chapter 3.4.3 showed that under certain conditions the POFC code can nevertheless reduce uncertainty for stimulus differences below the coarseness measure.
The main contribution of this thesis lies in the identification of parameters that influence the neural communication and the proposition and tests of two possible sources of the reference signals, interaction of the reference signal with the neural system and rules for a phase tag. Furthermore it was shown, that the position and the length of the encoding/decoding window have a strong effect on the mutual information calculation. Not anticipated was the fact, that the plots of influences of parameters are hardly ever "smooth". Though some mechanisms have been suggested to explain the performance of the codes and the reason behind the discontinuous relationship between stimulus difference and mutual information these mechanisms need to be checked more thoroughly. The varying performance of different setups for the phase code revealed, that the definition of the relevant properties has a strong influence. The mechanisms that enabled certain setups, for example te first first against the most spikes rule, to reach lower coarseness or higher accumulated difference remain to be revealed. In chapter 3.7 the whole setup was presented in a more organized manner, so that in following experiments one can hopefully "fail better". Using for example automated factorial experiments on all the parameters presented might deliver a model in which the phase code can reach a higher coarseness.

How do the results obtained here relate to the studies of Montemurro et al, who studied the real brain? Montemurro et al could show, that in the case of a monkey who was watching a video, regarding the phase of spikes in the visual cortex relative to fluctuations in the bands of the LFP can add up to 54% to the amount of information that is carried by those spikes. In the numerical experiments in this thesis differences on this order of magnitude could also be observed, though the reference signal had to be constructed artificially. Considering for example the differences in mutual information between RC and POFC for a given stimulus difference $\Delta I$ (plots on page 58) clearly shows that the phase-tag can add a considerable amount of information. However these results are not consistent and highly dependent on the exact stimulus difference $\Delta I$. Increasing the stimulus $I_2$ by another say 1 mV in some cases leads to the same $I_M$ for POFC and RC.
Fundamental differences in the experimental setup and the methods that are used to analyze the obtained data make it very hard to draw parallels between this thesis and the work of Montemurros et al.

Regarding the setup: While in Montemurro's case the stimulus was time-dependent and complex, stimulating a large number of neurons, in this thesis a simple static input current and just two neurons were used. This had an influence on the data that was obtained, the reference signal and therefore the $I_M$-calculations: the LFP as a reference is certainly to some extent driven by the time-dependent stimulus (video) while in this thesis the time-dependence of the artificially constructed reference signal does not stem from the time-dependence of the stimulus. Instead it arises solely from the time-constants (and other parameters) of the neural system. This then affects the assignment of phase tags to spikes, since the reference signals have obviously completely different sources.
Regarding the analysis of the obtained data: It was shown, that the $I_M$ calculations depend sensitively on the position and length of the decoding-window. In the supplements of Montemurro et al's work [12] the calculation of the mutual information is explained in more detail. There they also mention an influence of those two factors. The onset of the window is chosen by them to maximize the phase-information, the length of the window $\Delta t = 4ms$ in order to be able to compute phase coding information also for high-frequency bands of the LFP-fluctuation. Dividing the movie into very short time-bins of $\Delta t = 4ms$ leads to a large number ($\approx 90000$) of different stimuli but only a very small number of responses, since only very few spikes can occur in that interval. The simple model here has only two different stimuli $I_1$ and $I_2$ but some more possible responses.
One way of producing data with the simple model that fit into Montemurro et al's framework would be to use a time-varying reference signal and windows of similar size. The question of how to choose the time-dependence of the stimulus remains still remains open. The use of the small model can be to reveal mechanisms that lead to a reliable firing of spikes in a certain phase. But in order to use these results to understand the real brain it is absolutely neccessary to first more realistically model the LFPs, which are used as a reference signal. This might make it neccessary to use a larger model as Mazzoni et al [11] did.

## 5.1 Biological Plausibility

Is the two cell model biologically plausible? Or from a different perspective - Can the results obtained here be relevant for biological experiments? The system of two neurons is the most simple oscillating component of the large model by Mazzoni et al. [11] which was shown to resemble biologically observable LFP signals, therefore it might be. Integrate and fire neurons are widely used in neural modeling since they capture the essential properties of a neuron, the synapse model chosen is also commonly implemented. The parameters of the neurons and the synapses were similar to the ones found in the brain, the synapses might be a bit slow ($\tau_s = 10ms$) and do not resemble any particular kind (AMPA, GABA, etc), the LGN-neuron had to have a smaller time constant than the V1-neuron ($\tau_u = 20ms$ and $\tau_v = 60ms$) in order to cause oscillation, this fact that was not checked for plausibility. More questionable are the synaptic strengths ($w_{\text{ff}} = 1, w_{\text{fb}} = 8...20, w_{\text{ee}} = 6$ that were then chosen without regard to biological constraints, however the firing rates observed (10-60 Hz) are reasonable. LGN and V1 lie some cm apart, the time for signal propagation was modeled but included in the model ($t_{\text{delay}}$) and can be tested. The noisy neural "neighborhood" was only considered for the input-current into the LGN-neuron, one might extend the noise-input to the V1-neuron as well. The self-excitation that was introduced for the LGN-neuron because the analytical rate-model suggested it can easily

be explained by recurrent connections within LGN. Again one might consider to introduce the same kind of connections for the V1-neuron. Injecting a current into an LGN-neuron is not the best way to model visual input, but can be done in experiments[49]. Since Wei Wang et al. were able to identify LGN and V1 neurons with identical or similar receptive fields one should be able to choose neurons that correspond to the neurons in the two cell model. If it was possible to obtain recordings from both neurons for different strenghts of an input-current, one could run the same algorithms used here to calculate the coarseness and accumulated difference assuming rate and phase of firing code. Then one could also check whether the LFP-oscillations around the V1 neuron can be substituted by the oscillations of a single neuron itself. It would also be interesting to see if onset and length of the decoding window have a similar effect on the $I_M$ calculation using real neural recordings. To better understand the mechanisms behind the phase code, it is certainly easier to work with a small model, but of course its validity has to be confirmed.

## 5.2 Possible Improvements

Besides the the changes suggested for more biological relevance there are a number of improvements that can be made to the existing setup:

- Use a combination of membrane-potential/firing rate and synaptic activity as a reference signal.
- Try to further exploit the injected reference signal at different amplitudes.
- Use input from a Poisson process to a number of synapses instead of the direct input current + noise.
- Run experiments with more computational power to make more trials possible. Thereby the computed the relative frequency will be a better estimate of the probability distribution.
- Use a Hilbert-Transform (Matlab `hilbert`) to compute the instantaneous phase of spikes relative to the reference signal.
- Test the suggested mechanisms (chapter 15) more rigorously using interspike interval distributions and statistics for phase-distribution of the occurence of spikes. [2] might be helpful.
- Take the transmission delay between LGN and V1 into account. Signals need some time to propagate between those two areas.
- Use an analytically tracable model, for example FitzHugh-Nagumo instead of the I&F-model.
- Evaluate the effects of the time step $\Delta t$ of the numerical integration scheme.

[49] See [6] p. 31

# A Appendix

## A.1 Choice of a window function for the Fourier transformation

This part contains an important lesson that I learned for the application the Fourier transform on digital data. The effects encountered are called *spectral leakage*.
The continuous Fourier decomposition takes a signal $s(t)$ in the time domain and determines the coefficient of its decomposition into trigonometric (or complex exponential) functions with angular frequency $\omega$ $\mathcal{F}[s(t)](\omega) = \frac{1}{\sqrt{2\pi}} \int_{-\infty}^{\infty} exp(-i\omega x)s(x)dx$. Ideally the Fourier decomposition yields every frequency component contained in the signal. But because of sampling effects and finite recording time this is not so. Sampling effects (recording a signal with an instrument with limited temporal resolution $\Delta t$) are considered by multiplying $s(t)$ with a Dirac comb and are not relevant in the numerical simulation. The finite recording (simulation) time is relevant and can be described mathematically by multiplying $s(t)$ with a rectangular window function $w(t)$ that is 0 outside the recording-interval and 1 inside. Multiplication of the window function with the signal in the time-domain $\bar{s}(t) = w(t) \cdot s(t)$ is equivalent to convolution in the frequency domain $\mathcal{F}(s(t)w(t)) = \mathcal{F}(w(t)) * \mathcal{F}(s(t))$. The Fourier decomposition of a rectangular window looks like this[50]:

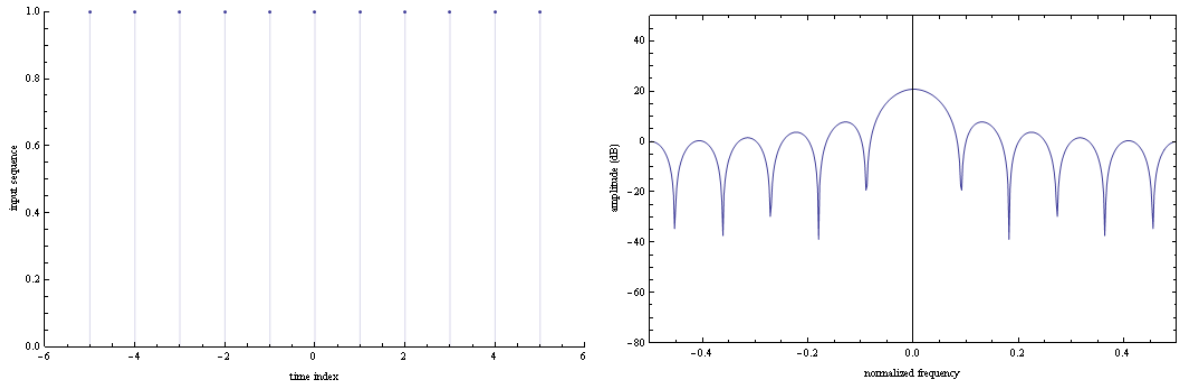


Figure 19: Fourier decomposition of a rectangular window.

This leads to artefacts in the Fourier decomposition, called spectral leakage. Frequency components that are close together cannot be distinguished anymore. An ideal window function would be a Dirac impulse in the frequency domain, but this is not possible for finite-sized windows. Therefore one has to choose between increased frequency resolution - signal components with similar frequencies and similar strength can be distinguished or dynamic range (detecting a small signal in the presence of noise). Characteristics that are of importance when choosing a window function are

1. width of the main lobe (the narrower the higher the frequency resolution)
2. attenuation of the maximum of the first side lobe (the narrower the better the noise suppression)

[50] Used an applet from `http://demonstrations.wolfram.com/DiscreteFourierTransformOfWindowingFunctions/` by Siva Perla.

Since rate oscillations are noisy but only occur at one rate the noise suppression is favored. This suggests the use of a Hann window. This window is created by MATLAB command `hann`.

## A.2 Parameters used for the rate code

| | |
|---|---|
| Trials | 500 per $I_2$ |
| $\sigma$ | 2, 5, 10, 15 mV |
| $w_{\text{fb}}$ | 8, 10, 12, 14 |
| $w_{\text{ee}}$ | 6 |
| $I_1$ | 35 mV |
| $I_2$ | 35 mV ... 65 mV |
| $T$ | 77 ms |
| $T_{\text{start}}$ | 462 ms |
| $\Delta t$ | 0.05 ms |

Table 28: Parameters for the test of the rate code.

## A.3 Parameters used for determining a POF code setup

| | |
|---|---|
| Osc. Periods | 1 |
| Osc. Freq | Fixed, 12.99 Hz, T = 77 ms |
| $T_{\text{start}}$ | 462 ms |
| Phase Rule | Most Spikes |
| fb | 10 |
| $\sigma$ | 5 mV |
| $\Delta I$ | 0 ... 30 mV |
| $I_1$ | 35 mV |
| Trials | 500 trials per $\Delta I$ |
| Amplitude Ref. Sig | 4 mV |
| Noise Ref. Sig | 0mV |

Table 29: Settings used for non-influencing reference signal vs injected reference signal.

| | |
|---|---|
| Osc. Periods | 1 |
| Osc. Freq | Fixed, 12.99 Hz, T = 77 ms |
| $T_{\text{start}}$ | 462 ms |
| Phase Rule | Most Spikes |
| Ref. Sinal | Non influencing |
| fb | 10 |
| $\sigma$ | 5 mV |
| $\Delta I$ | 0 ... 30 mV |
| $I_1$ | 35 mV |
| Trials | 500 trials per $\Delta I$ |
| Amplitude Ref. Sig | 4 mV |
| Noise Ref. Sig | 0mV |

Table 30: Settings used for first spike tag vs most spikes tag.

| | |
|---|---|
| Osc. Periods | 1 |
| Osc. Freq | Fixed, 12.99 Hz, T = 77 ms, adapting acc. to chapter 3.2.3 |
| Phase Rule | First Spike |
| Ref. Sinal | Non influencing |
| fb | 10 |
| $\sigma$ | 5 mV |
| $\Delta I$ | 0 ... 30 mV |
| $I_1$ | 35 mV |
| Trials | 500 trials per $\Delta I$ |
| Amplitude Ref. Sig | 4 mV |
| Noise Ref. Sig | 0mV |

Table 31: Settings used for fixed frequency vs adapting frequency.

| | |
|---|---|
| Osc. Periods | 1, 2, 3 |
| Osc. Freq | fixed, 12.99Hz, T = 77ms |
| Phase Rule | First Spike |
| Ref. Sinal | Non influencing |
| fb | 10 |
| $\sigma$ | 5 mV |
| $\Delta I$ | 0 ... 30 mV |
| $I_1$ | 35 mV |
| Trials | 500 trials per $\Delta I$ |
| Amplitude Ref. Sig | 4 mV |
| Noise Ref. Sig | 0mV |

Table 32: Settings used for single period vs multiple periods.

## A.4 MATLAB functions

Unfortunately the u- and v-neurons in the thesis are called v- and w-neuron in the MATLAB functions.

**CoupledIF**

Simulates the time course of the two coupled I&F neurons.
Input:

- I_input – vector of length(SimTime/delta_t+1) containing the time course of the input current, in mV
- I_sigma – strength of noise, in mV
- SimTime – length of Simulation, in msec
- delta_t – time step of the simulation, in msec
- use_p – boolean, experimental, use randomly generated Poisson input
- tau_input – time constant of the synapse for Poisson input
- fb – strength of the feedback connection, in dimensionless units
- ee – strength of the self-excitation, in dimensionless units
- tau_w – time constant of the neuron in V1 receiving excitation, in msec
- w_input – vector of length(SimTime/delta_t+1) containing the time course of reference signal that is to be injected into the cell
- w_sigma – strength of the noise added to the reference signal

Output:

- v, w – objects of type IFNeuron. Contains v – timcourse of length(SimTime/delta_t+1), v_reset – reset potential, v_th – threshold potential, tau – membrane time constant, r_m membrane resistance, E_L equilibrium potential, E_S synaptic potential, v_spike - voltage for a spike
- ff_syn, fb_syn, ee_syn, p_syn – vectors of length(Simtime/delta_t+1) containing the time course of the synaptic input to the feedforward, feedback, self-excitatory and Poisson-input synapse
- inp_c – vector of length(Simtime/delta_t+1) containing the time course of the given direct input (including noise) for the v-neuron.

**Calculate_IM**

Calculates the mutual information for a number of trials and stimuli.
Input:

- Recordings – (Number of Stimuli x Number of Trials) array containing integers that stand for the neural reaction

Output:

- IM – mutual information
- CondProbPlot – conditional probabilites as a function of the reaction index

**MainFreqComponent**
Determines the main frequency component (component with highest power) in a signal using a Fourier decomposition.
Input:

- signal – vector containing the signal to be analyzed
- Fs – sampling frequency in samples/sec

Output:

- freq – main frequency component, in Hz up to the Nyquist frequency
- fourier – vector containing the fourier coefficients

**DeltaI_IM_Plot**
Creates the $\Delta I$–$I_M$ plots for phase of firing and rate code used in this thesis. $I_1$ is 35 mV.
Input:

- I2_max – maximum value for the second input current
- mfreqcomp – vector containing the main frequency components of the rate oscillation to create an appropriate reference signal, in Hz

Output:

- Im_RC – vector containing the mutual information for each pair of $I_1$ and $I_2$ for $I_2$ starting at $I_1$ up to I2_max calculated assuming a rate code
- Im_POFC – vector containing the mutual information for each pair of $I_1$ and $I_2$ for $I_2$ up to I2_max calculated assuming a phase of firing code

**PhaseDistribution**
Determines the number of spikes occuring in each phase of a spike train, used for the most spikes phase tag.
Input:

- STrain – spike train containing 0 for no spike, 1 for spike occured
- delta_t – time step width of the numerical simulation, in msec
- Freq – frequency of the reference signal, in Hz
- NPhases – number of phases into which the spike train is to be divided, at least 1

Output:

- p – vector length(NPhases), containing the number of spikes that occured in each phase

**Two_Cell_Model_Plots_Script**
Contains various scripts to create firing rates from spike trains and plot Fourier-decompositions.
Input: –
Output: –

## A.5 MATHEMATICA script

```
In[20]:= w_fb = 10;
         α_u = 1;
         α_v = 1;
         w_ee = 1.5;
         w_ii = 0;
         w_ff = 1;
         τ_u = 1;
         s =
          {{(α_u w_ee - 1) / Subscript[τ, u], -Subscript[α, u] Subscript[w, fb] / Subscript[τ, u]},
           {Subscript[α, v] Subscript[w, ff] / Subscript[τ, v],
            (-α_v w_ii - 1) / Subscript[τ, v]}}
         a = Simplify[Eigenvalues[s]]
         Plot[{Re[First[a]], Re[Last[a]]}, {τ_v, 0, 20}, AxesLabel → {τ_v, Re[λ_1,2]},
          AxesOrigin → {0, 0}, PlotLabel → "w_fb=xx"]
```

# References

[1] Scholarpedia. Checked 2010/06/29.

[2] A. N. Burkitt. A review of the integrate-and-fire neuron model: I. homogeneous synaptic input. *Biological Cybernetics*, 2006.

[3] Francois Chapeau-Blondeau and Nicolas Chambet. Synapse models for neural networks: From ion channel kinetics to multiplicative coefficient w-ij. *Neural Computation*, 7:713–734, 1995.

[4] Thomas M. Cover and Joy E. Thomas. *Elements of Information Theory*. Wiley, 2006.

[5] Mike Dawson. `http://www.bcp.psych.ualberta.ca/~mike/Pearl_Street/Dictionary/contents/C/coarsecode.html`.

[6] Peter Dayan and L. F. Abbott. *Theoretical Neuroscience*. The MIT Press, 2001.

[7] Prof. Dirk Ferus. *Differentialgleichungen für Ingenieure, Skript*. TU Berlin, 09.02.2007.

[8] Wulfram Gerstner and Werner M. Kistler. *Spiking Neuron Models*. Cambridge University Press, Online Verison, 2002.

[9] D. Hansel, G. Mato, C. Meunier, and L. Neltner. On numerical simulations of integrate-and-fire neural networks. *Neural Computation*, Vol 10; Nb 2:467–484, 1998.

[10] Harro Heuser. *Gewöhnliche Differentialgleichungen - Einführung in Lehre und Gebrauch*. B. G. Teubner Stuttgart, 1995.

[11] Alberto Mazzoni, Stefano Panzeri, Nikos K. Logothetis, and Nicolas Brunel. Encoding of naturalistic stimuli by local field potential spectra in networks of excitatory and inhibitory neurons. *Computational Biology*, Vol 4, Iss 12, 2008.

[12] Marcelo A. Montemurro, Malte J. Rasch, Yusuke Murayama, Nikos K. Logothetis, and Stefano Panzeri. Phase-of-firing coding of natural visual stimuli in primary visual cortex. *Current Biology*, Vol 18, N 5:375–380, 2008.

[13] Douglas C. Montgomery and George C. Runger. *Applied Statistics and Probability for Engineers*. John Wiley and Sons, Inc., 2003, 3rd Ed.

[14] Alan V. Oppenheim, Alan S. Willsky, and Ian T. Young. *Signals and Systems*. Prentice-Hall, 1983.

[15] George Orwell. Politics and the english language. *http://www.george-orwell.org/Politics_and_the_English_Language/0.html*, 1946.

[16] Stefano Panzeri, Nicolas Brunel, Nikos K. Logothetis, and Christoph Kayser. Sensory neuroal codes using multiplexed temporal scales. *Trends in Neurosciences, in review*, 2010.

[17] William H. Press, Saul A. Teukolsky, William T. Vetterling, and Brian P. Flannery. *Numerical Recipes in C*. Cambridge University Pr., 3rd ed., 2007.

[18] Dale Purves, editor. *Neuroscience*. Sinauer Associates, Inc., 2004, 3rd Ed.

[19] Fred Rieke, David Warland, Rob de Ruyter van Stevenick, and William Bialek. *Spikes - Exploring the Neuroal Code*. The MIT Press, 1996.

[20] Inés Samengo and Marcelo A. Montemurro. Conversion of phase information into a spike-count code by bursting neurons. *PLoS One*, Vol 5, Iss 3, 2010.

[21] Claude Shannon. A mathematical theory of communication. *The Bell Systems Technical Joural*, 27:379–423, 1948.

[22] Bernard Sonnenschein. *Kleine Netzwerke aus Erregbaren Elementen: Modellierung der Neurodynamik, Bachelor's Thesis*. HU Berlin, 2008.

[23] Steven Strogatz. *Nonlinear Dynamics and Chaos*. Perseus Books, 1994.

[24] Steven P. Strong, Roland Koberle, Rob R. de Ruyter van Stevenick, and William Bialek. Entropy and information in neural spike trains. *Physical Review Letters*, 80:197–200, 1998.

[25] Wim van Drongelen. *Signal Processing for Neuroscientists*. AP, 2006.

[26] Wei Wang, Helen E Jones, Ian M Anolina, Thomas E Salt, and Adam M Silito. Functional alignment of feedback effects from visual cortex to thalamus. *Nature Neuroscience*, 9:1330–1336, 2006.

# Eigenständigkeitserklärung

Hiermit versichere ich, dass ich die vorliegende Arbeit selbständig verfasst und keine anderen als die angegebenen Quellen und Hilfsmittel verwendet habe.

Maximilian Thess